

A Charge Separation Study to Enable the Design of a Complete Cooling Channel

*Work supported in part by DOE STTR grant DE-SC 0007634.

Outline

- Motivation & Goals
- Overview
- The Study
- Suggestions to improve next iteration of designing the Charge Separator
- Summary & Future

Preliminaries

- This work was supported under a phase II STTR grant with JLAB announced 3/4/13 with start date 4/22/13.
- We have weekly meetings with attendance and/or input by:
 - Slava Derbenev (JLAB subgrant PI), Vasiliy Morozov, Rol Johnson, Chuck Ankenbrandt, Dave Neuffer, Katsuya Yonehara, Jim Maloney, & Cary Yoshikawa (MuPlus PI)

Motivation & Goals

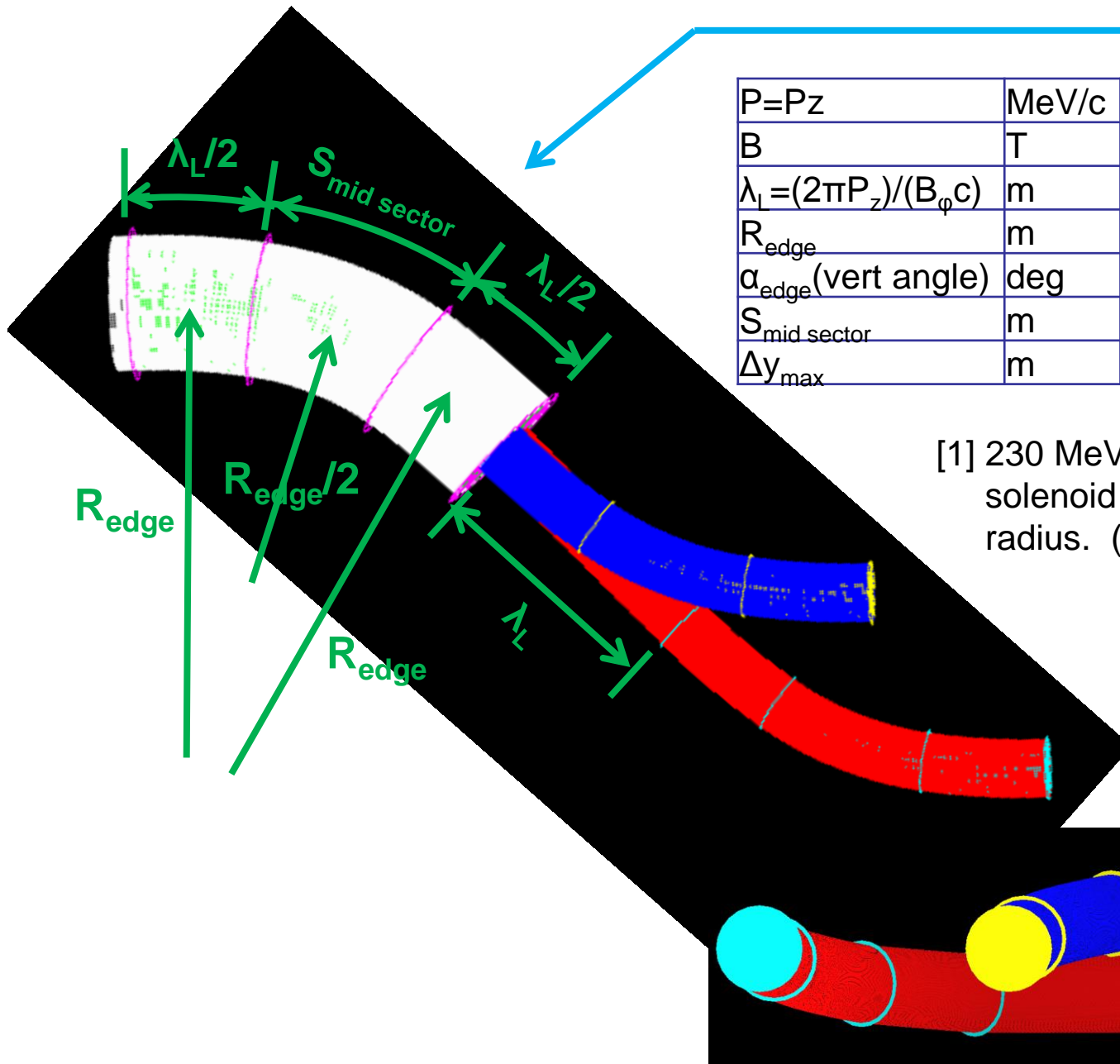
- Within the context of the HCC Complete Cooling Channel, our interest is to obtain particle distributions that possess the effects of having gone through a charge splitter, since this is necessary for the HCC.
- Our goal is not to design the charge splitter, but rather to extract particle distributions that provide the starting point in designing the complete cooling channel.

Secondary Benefits:

- The resultant particle distributions might serve as a basis upon which the various 6D cooling channels may use as input for performance comparisons between the options that apply to a single charge sign.
- Lessons learned can be fed back into the design of a real charge separator.

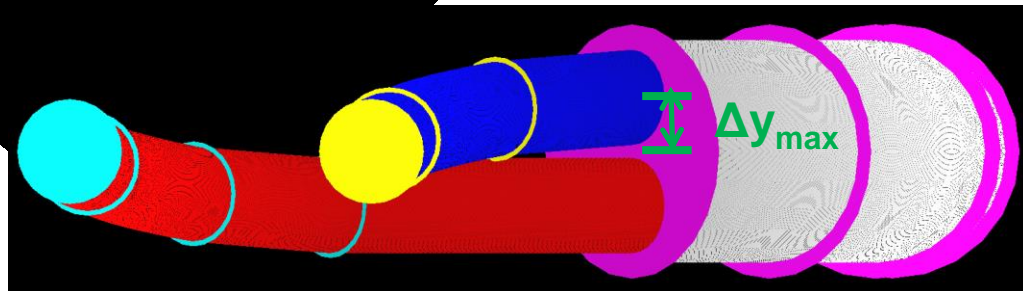
Overview

- Started from design using bent solenoids by Palmer & Fernow [PAC11 MOP001] and created a configuration (on spreadsheet) that might work without need for acceleration at 250 MeV/c.
- Simulations in ICOOL of the 250 MeV/c design showed promising results.
- G4BL was used to validate and determine limits of non-overlapping volumes of reverse bends in splitter.
- Implementation of the charge splitter in G4BL revealed some unexpected effects that resulted in a design of a pseudo charge splitter, whose purpose is to generate the sought after simulated particles.
- The pseudo charge splitter was optimized using G4BL for 250 MeV/c.
- Scrutiny of the charge splitter output revealed distortion of the longitudinal dynamics that resulted in losses during RF capture following the splitter.
- RF gymnastics upstream of the charge splitter effectively eliminates losses in the downstream RF capture and even raises the efficiency at the splitter exit!



| P=Pz | MeV/c | 230[1] | 250 | 300 | 400 |
|-------------------------------------|-------|--------|-------|-------|-------|
| B | T | 3 | 2 | 1.9 | 1.9 |
| $\lambda_L = (2\pi P_z)/(B_\phi c)$ | m | 1.61 | 2.62 | 3.31 | 4.41 |
| R _{edge} | m | 2.5 | 7.36 | 6.67 | 12.39 |
| α_{edge} (vert angle) | deg | 5.86 | 3.24 | 4.52 | 3.24 |
| S _{mid sector} | m | 1.6 | 1.7 | 0.45 | 0.8 |
| Δy_{max} | m | 0.165 | 0.340 | 0.332 | 0.340 |

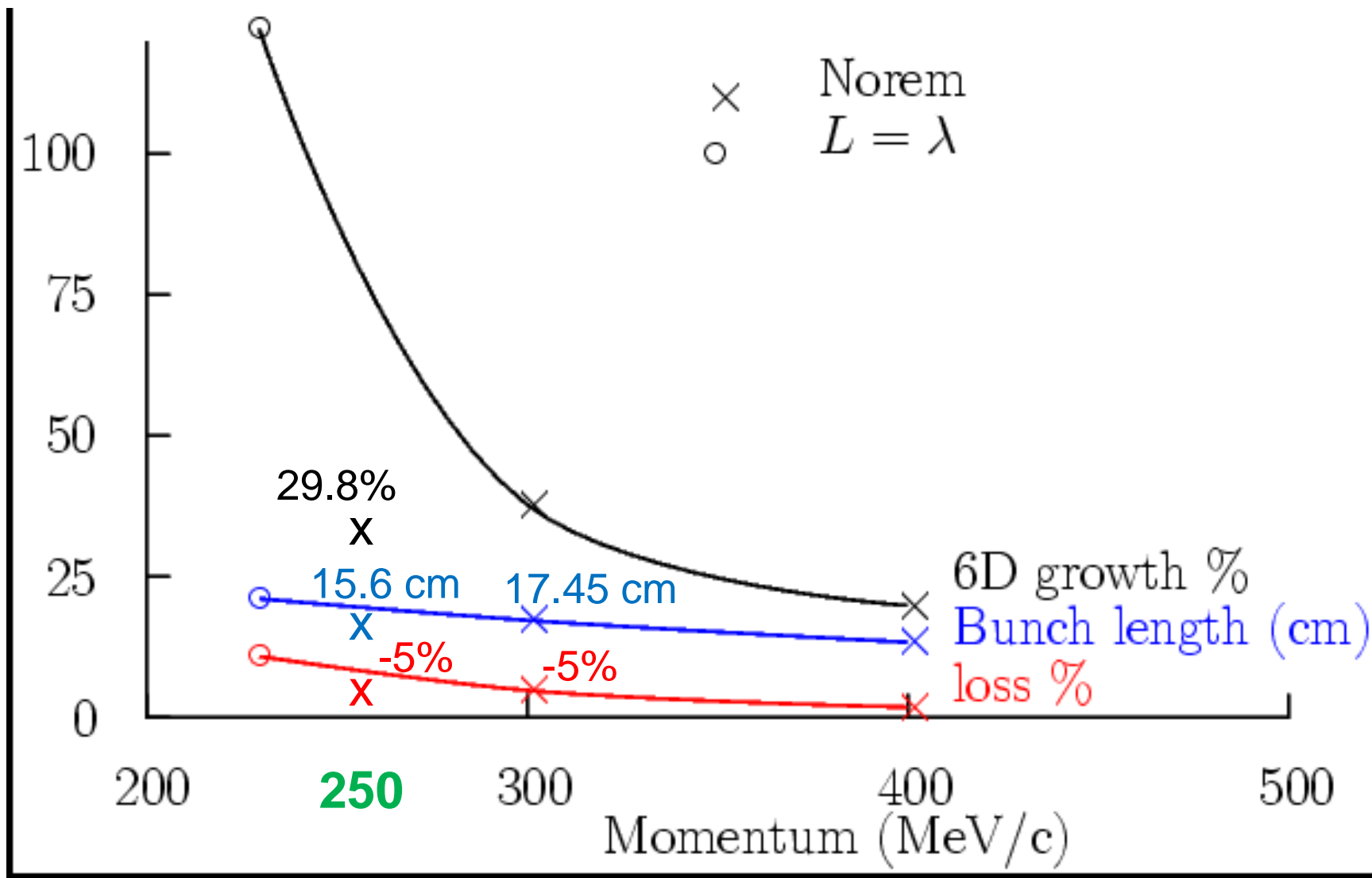
[1] 230 MeV/c case is a bent solenoid using a single radius. (no mid sector)



Results of Palmer/Fernow Study and Current One at 250 MeV/c using ICOOL

| P (MeV/c) | Init | Init | Neg | Pos | <incr> % |
|--------------|-----------------------------|--------------------|--------|--------|------------------------------------|
| 230 | ϵ_{\perp} (mm) | 15.1 | 17.6 | 21.1 | 28% |
| | ϵ_{\parallel} (mm) | 43.9 | 59.7 | 82.1 | 61% |
| | σ_{ct} (mm) | 111 | 151 | 218 | 66% |
| | Trans (%) | 100 | 85 | 89 | -13% |
| 250 | ϵ_{\perp} (mm) | 15.54(-)/15.67(+)* | 15.56 | 15.84 | 0.13(-) / 1.08(+) / 0.61%(avg.) |
| | ϵ_{\parallel} (mm) | 27.71(-)/30.15(+)* | 33.22 | 41.44 | 19.88(-) / 37.45(+) / 28.67%(avg.) |
| | σ_{ct} (mm) | 90.1(-)/94.4(+)* | 141.26 | 171.03 | 56.78(-) / 81.18(+) / 68.98%(avg.) |
| | Trans/20kPOT | 4553(-)/4540(+)* | 4371 | 4272 | -4.00(-) / -5.90(+) / -4.95%(avg.) |
| 300 | ϵ_{\perp} (mm) | 15.1 | 15.4 | 16.7 | 6% |
| | ϵ_{\parallel} (mm) | 38.1 | 45.8 | 50.3 | 26% |
| | σ_{ct} (mm) | 102 | 162 | 187 | 66% |
| | Trans (%) | 100 | 95 | 95 | -5% |
| 400 | ϵ_{\perp} (mm) | 15.1 | 15.2 | 15.3 | 1% |
| | ϵ_{\parallel} (mm) | 38.1 | 43.8 | 47.8 | 20% |
| | σ_{ct} (mm) | 102 | 134 | 162 | 45% |
| | Trans (%) | 100 | 98 | 97 | -2.5% |

* Initial particle distributions are end of Neuffer 325 MHz Rotator.



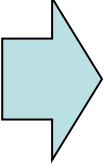
Simulations of 250 MeV/c Configuration

| | ϵ_T | | ϵ_L | | ϵ_{6D} | | N_{survive} | |
|---------------------------------------------------|--------------|---------|--------------|---------|-----------------|---------|----------------------|---------|
| units | mm-rad | | mm | | mm ³ | | per 20k POT | |
| Particle Species | μ^+ | μ^- | μ^+ | μ^- | μ^+ | μ^- | μ^+ | μ^- |
| At End of Rotator | 15.66 | 15.54 | 30.06 | 27.71 | 7368 | 6690 | 4536 | 4553 |
| End of Charge Splitter post Rotator (ICOOL) | 15.84 | 15.56 | 41.44 | 33.22 | 10,360 | 7964 | 4272 | 4371 |
| 4D Cooler End | 6.381 | 6.380 | 27.83 | 25.89 | 1133 | 1053 | 3642 | 3697 |
| 4D Cooler Match End* | 6.673 | 6.730 | 29.56 | 27.98 | 1315 | 1266 | 3586 | 3659 |
| Charge Split End aft 4D Cool Match End (ICOOL) | 7.224 | 7.207 | 65.99 | 62.06 | 3420 | 3210 | 3742 | 3781 |
| Acceptance of Katsuya's HCC | 20.4 | | 42.8 | | 12,900 | | | |

*Lattice of the matching section out of the 4D Cooler ($\pm 2.8T \rightarrow 2T$) was the mirror image of that used to match into the 4D Cooler ($2T \rightarrow \pm 2.8T$).

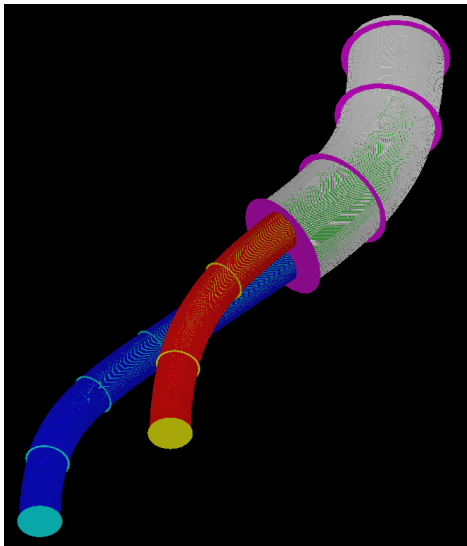
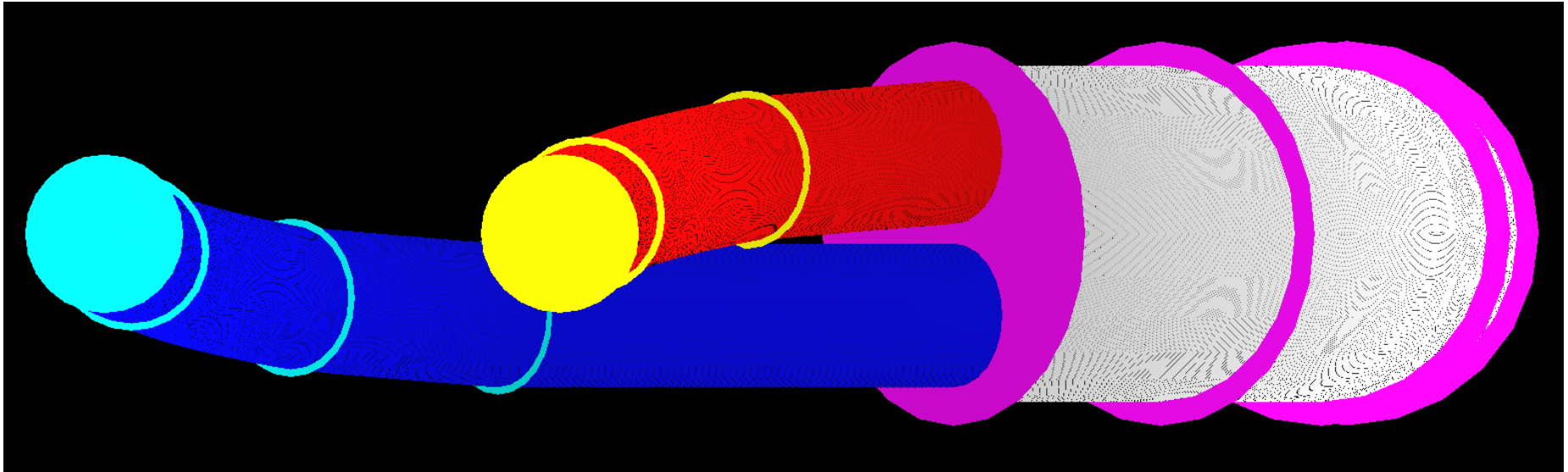
Ecalc9f cuts: (Effectively only momentum)

- $175 \text{ MeV/c} < p < 375 \text{ MeV/c}$
- $A_{\text{trans}} < 1\text{m}$, $A_{\text{long}} < 0.92244 \text{ m} \leftarrow$ none for 325 MHz

 **Muons out of the 250 MeV/c charge splitter following the Rotator should fit into the HCC!**

What are the geometric constraints for the downstream segments to not overlap each other?

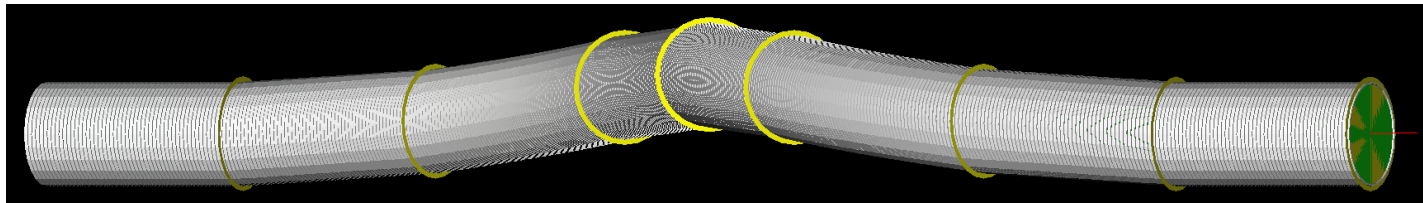
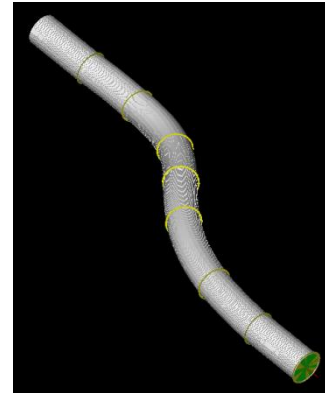
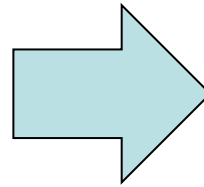
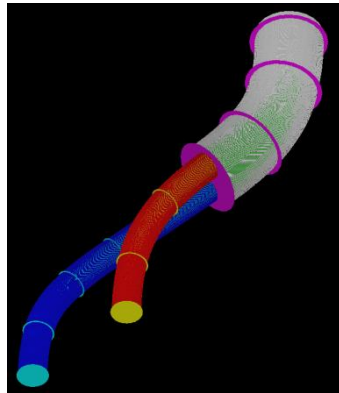
Study in Geometric Constraints (non-overlapping volumes)



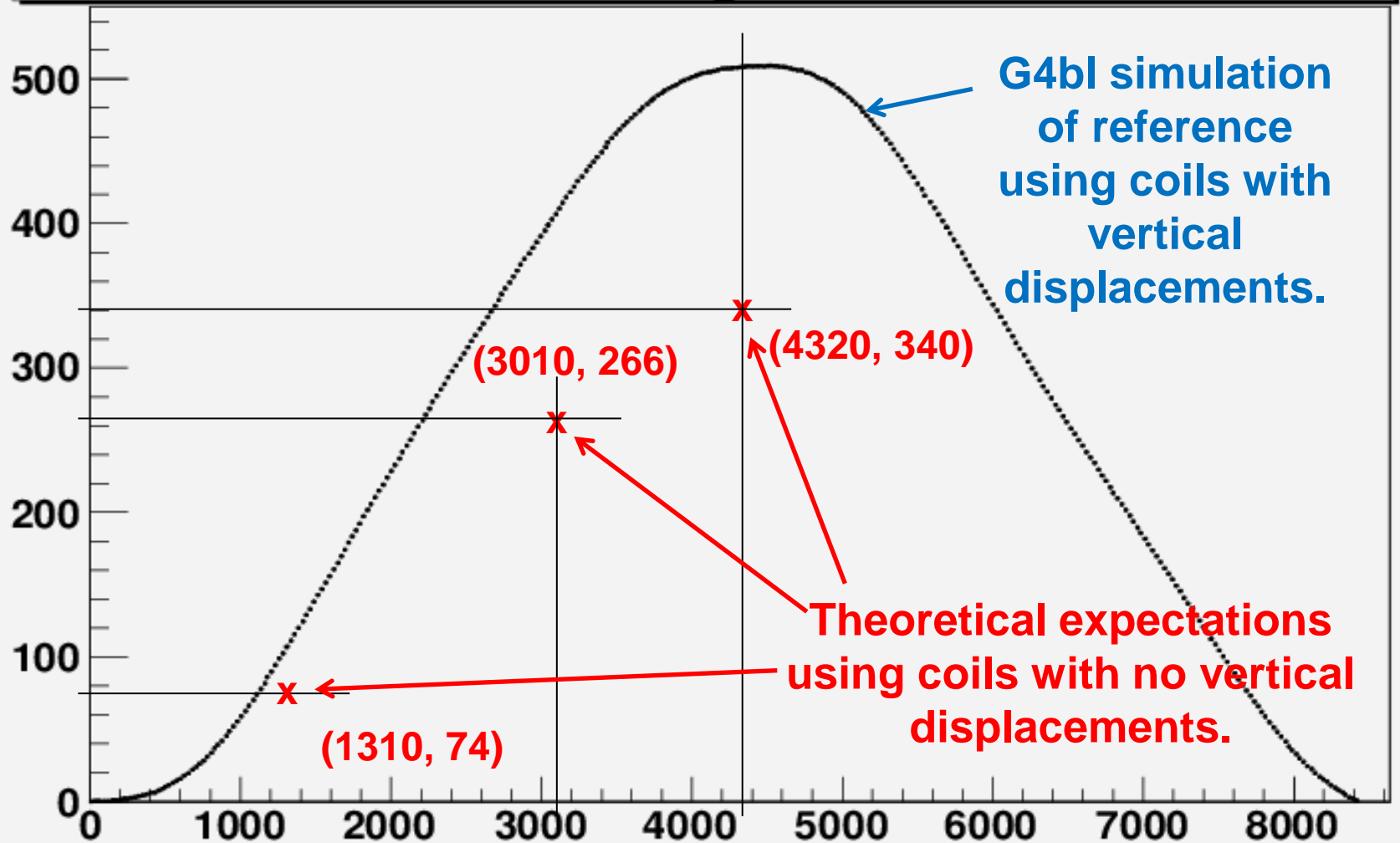
| P_{ref} of Bent Solenoid (MeV/c) | $R_{\text{outer, max}}$ (cm) |
|---------------------------------------------------|---------------------------------|
| 250 (design highlighted in previous slides) | 30 |
| 400 (Palmer/Fernow design in PAC11 MOP001) | 29 |

Pseudo Charge Splitter Design

- Recall our goal is to obtain distributions indicative of that having gone through a charge splitter.
- To avoid complexities of the transition region at end of first bend, we simply simulated a continuous channel for each sign.
 - Similar strategy as performed in earlier studies by Palmer/Fernow using ICOOL.



y vs. $\sqrt{276.142958 \cdot t \cdot 276.142958 \cdot t - y \cdot y}$
 Ref Mu- in Charge Separator w/ forward & reverse bends
 $P=250\text{MeV}/c$ $B=2.0\text{T}$ $R_{\text{edge}}=7.36\text{m}$ $L_{\text{center}}=1.7\text{m}$

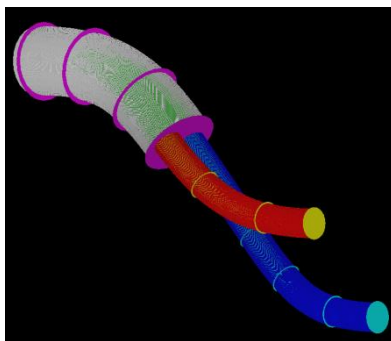


In analyzing the effect of a charge splitter, we prefer to have a configuration that has an analytic description against which we can validate our simulations.

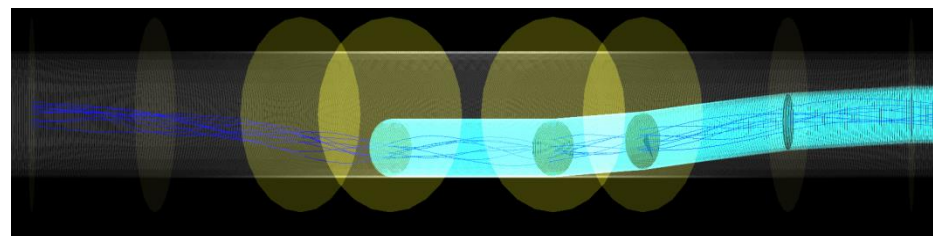
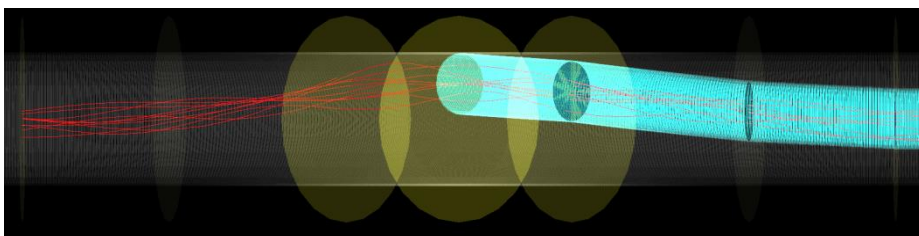
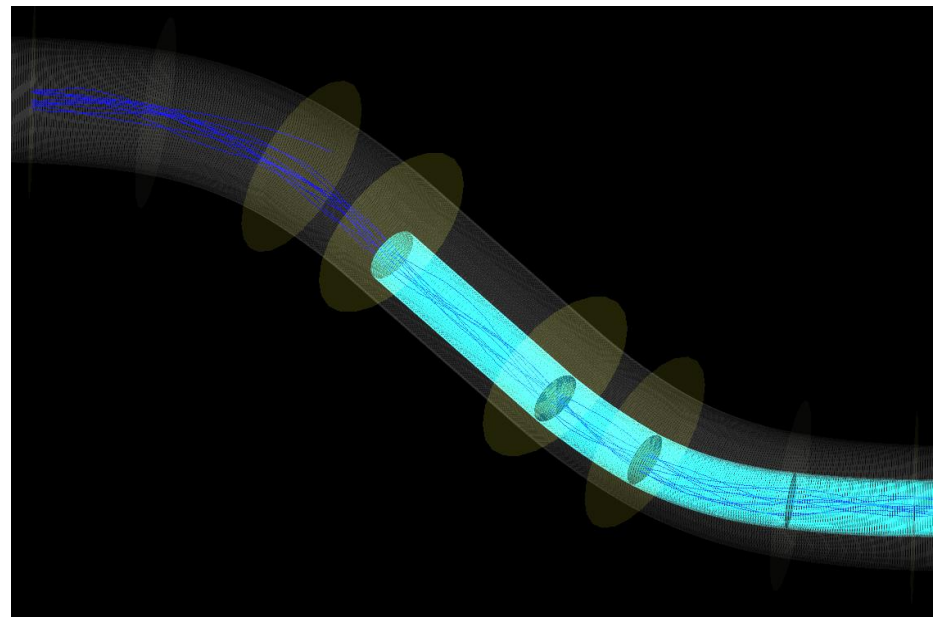
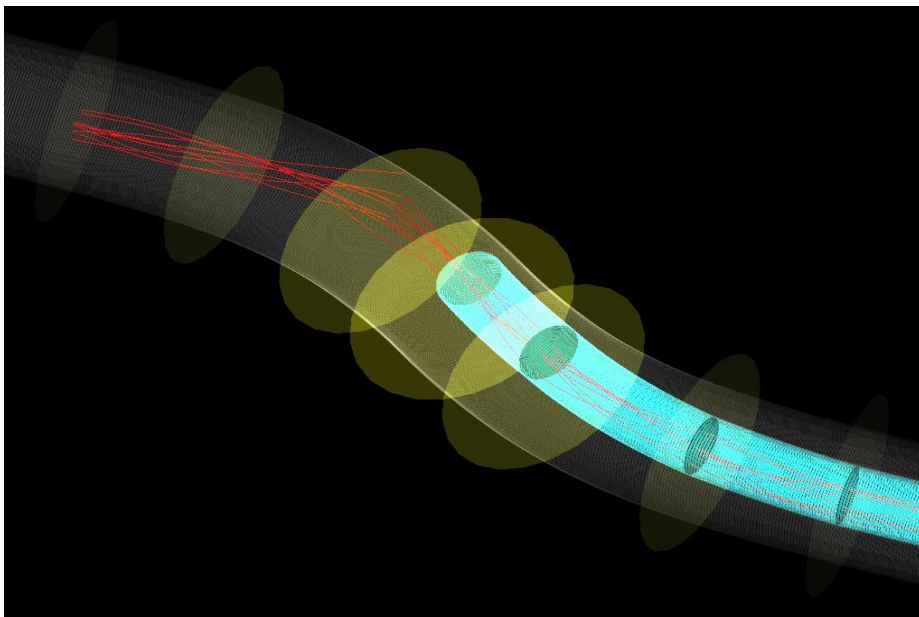
Fastest way to obtain desired distributions:

- Use large aperture “flat” bent solenoids that are constrained to lie in the horizontal plane to generate the appropriate fields.**
- Use limiting apertures to extract effect of scraping from coils.**

Mu-'s



Mu+'s



| | ϵ_T | | ϵ_L | | ϵ_{6D} | | N_{survive} | |
|---------------------------------------------------|--------------|---------|--------------|---------|-----------------|---------|----------------------|---------|
| units | mm-rad | | mm | | mm ³ | | per 20k POT | |
| Particle Species | μ^+ | μ^- | μ^+ | μ^- | μ^+ | μ^- | μ^+ | μ^- |
| At End of Rotator | 15.66 | 15.54 | 30.06 | 27.71 | 7368 | 6690 | 4536 | 4553 |
| End of Charge Splitter post Rotator (ICOOL) | 15.84 | 15.56 | 41.44 | 33.22 | 10,360 | 7964 | 4272 | 4371 |
| End of Charge Splitter post Rotator (G4BL) | 15.20 | 15.29 | 39.32 | 35.37 | 9051 | 8215 | 4282 | 4463 |
| 4D Cooler End | 6.381 | 6.380 | 27.83 | 25.89 | 1133 | 1053 | 3642 | 3697 |
| 4D Cooler Match End | 6.673 | 6.730 | 29.56 | 27.98 | 1315 | 1266 | 3586 | 3659 |
| Charge Split End aft 4D Cool Match End (ICOOL) | 7.224 | 7.207 | 65.99 | 62.06 | 3420 | 3210 | 3742 | 3781 |
| Charge Split End aft 4D Cool Match End (G4BL) | 7.154 | 6.855 | 60.40 | 38.16 | 3075 | 1787 | 3726 | 3481 |
| Acceptance of Katsuya's HCC | 20.4 | | 42.8 | | 12,900 | | | |

scraping?

Ecalc9f cuts: (Effectively momentum only)

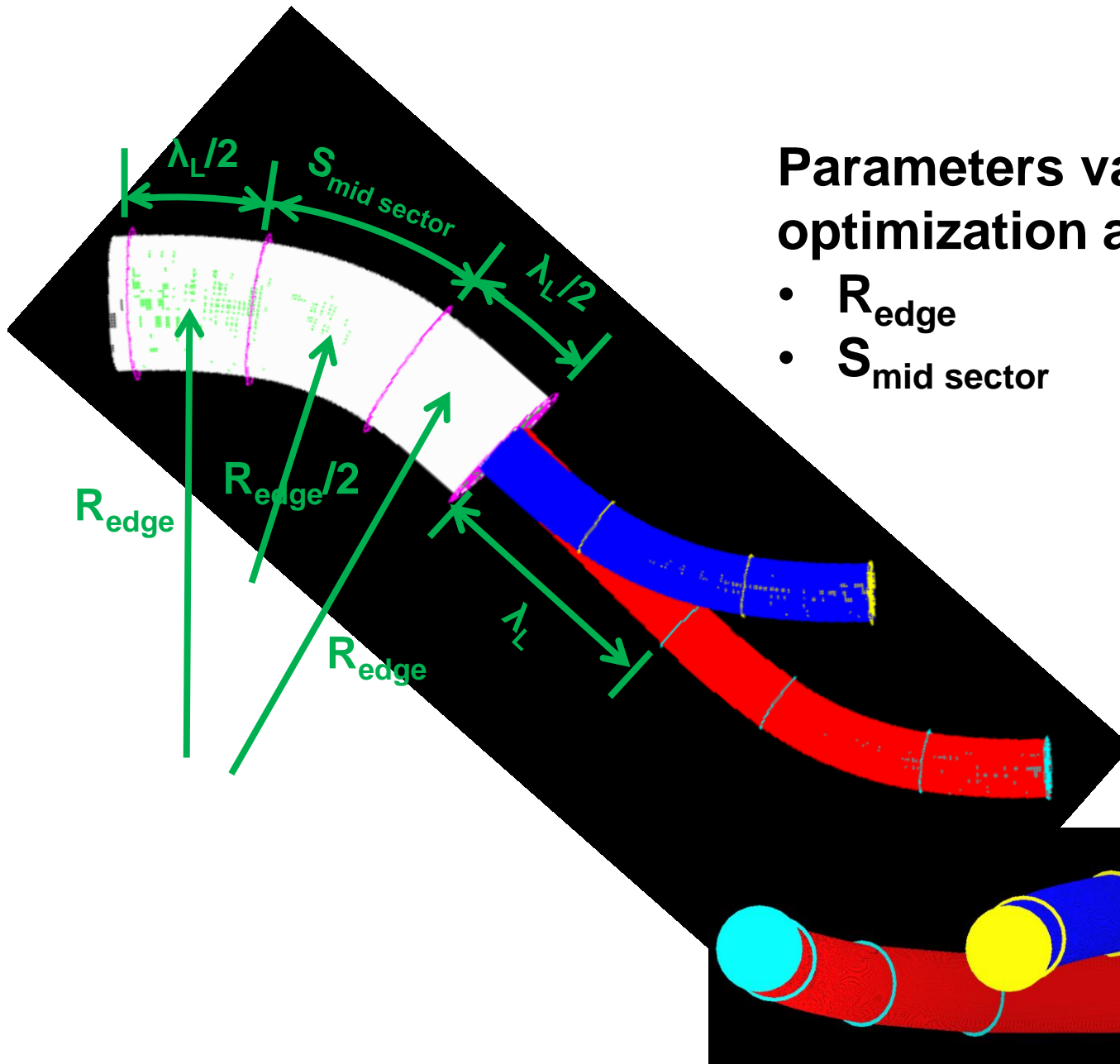
- $175 \text{ MeV/c} < p < 375 \text{ MeV/c}$
- $A_{\text{trans}} < 1\text{m}$, $A_{\text{long}} < 0.92244 \text{ m}$ ← none for 325 MHz

Optimization for 250 MeV/c

Can we do better?

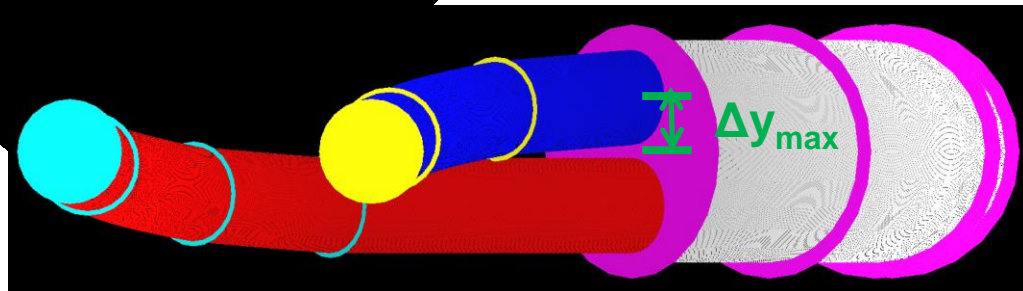
Note that the initial configuration for 250 MeV/c was designed to have the same vertical pitch angle for the reference as the 400 MeV/c case, since that had the best performance.

| P=Pz | MeV/c | 230[1] | 250 | 300 | 400 |
|-------------------------------------|-------|--------|-------|-------|-------|
| B | T | 3 | 2 | 1.9 | 1.9 |
| $\lambda_L=(2\pi P_z)/(B_\phi c)$ | m | 1.61 | 2.62 | 3.31 | 4.41 |
| R_{edge} | m | 2.5 | 7.36 | 6.67 | 12.39 |
| α_{edge} (vert angle) | deg | 5.86 | 3.24 | 4.52 | 3.24 |
| $S_{\text{mid sector}}$ | m | 1.6 | 1.7 | 0.45 | 0.8 |
| Δy_{max} | m | 0.165 | 0.340 | 0.332 | 0.340 |



Parameters varied in this optimization are:

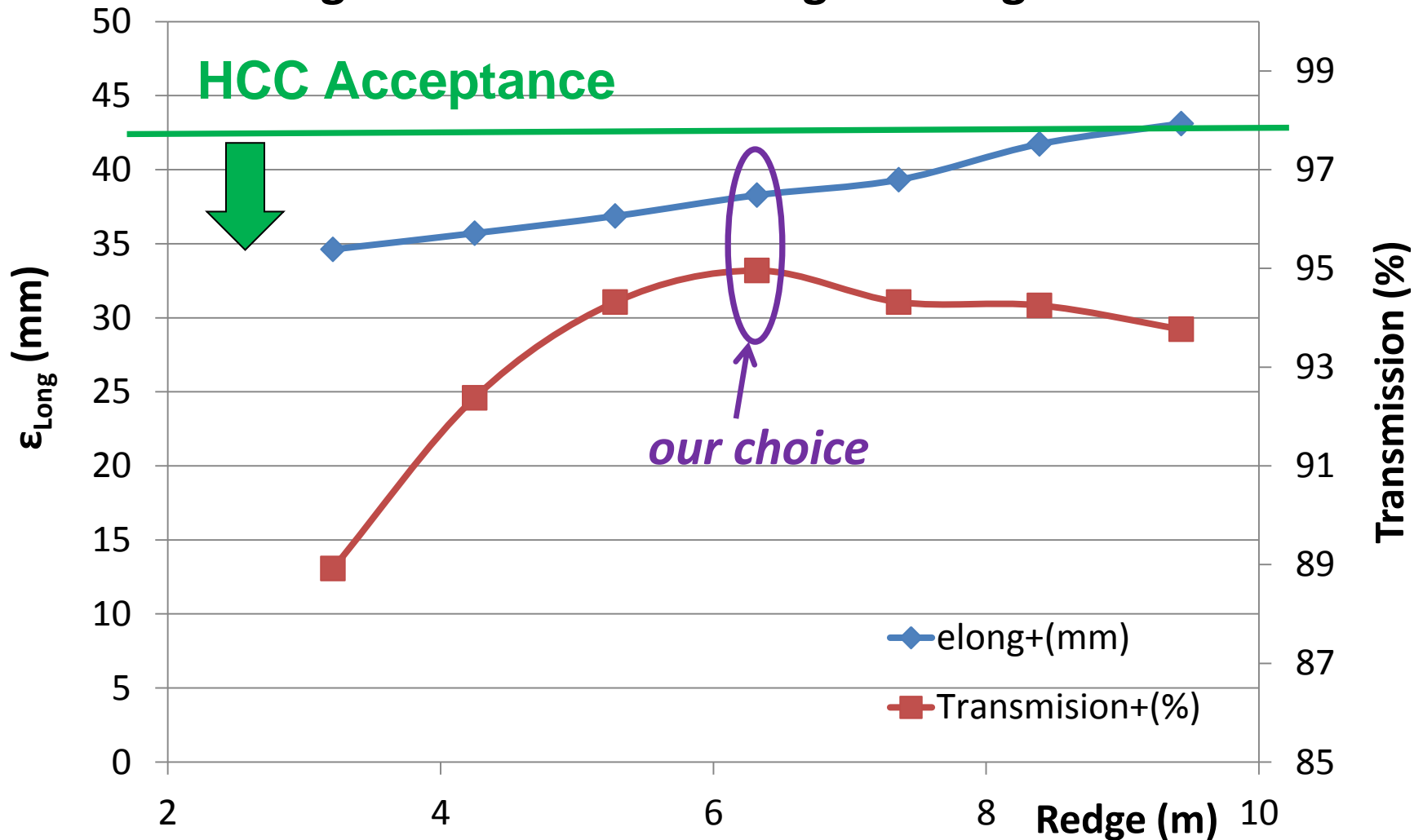
- R_{edge}
- $S_{\text{mid sector}}$



| | | | | | | | | |
|-------------------------------------|-------|-------|------|------|-------|-------|-------|-------|
| $P=P_z$ | MeV/c | 250 | | | | | | |
| B | T | 2 | | | | | | |
| $\lambda_L=(2\pi P_z)/(B_\phi c)$ | m | 2.62 | | | | | | |
| R_{edge} | m | 3.21 | 4.25 | 5.28 | 6.32 | 7.36 | 8.39 | 9.43 |
| α_{edge} (vert angle) | deg | 7.4 | 5.6 | 4.5 | 3.8 | 3.2 | 2.8 | 2.5 |
| $S_{\text{mid sector}}$ | m | 0 | 0.42 | 0.85 | 1.27 | 1.70 | 2.13 | 2.55 |
| Δy_{max} | m | 0.342 | | | | | | |
| $S_{\text{Longer Channel}}(+)$ | m | 7.86 | 8.71 | 9.56 | 10.41 | 11.26 | 12.11 | 12.96 |

Optimization is performed on the longer channel (+’s), since the longitudinal growth (no RF) drives the acceptance.

Transmission Efficiency and $\epsilon_{\text{Longitudinal}}$ for Positively Charged Particles Traversing the Longer Path



Current Results using G4beamline

(only considered post phase rotator)

| | ϵ_T | | ϵ_L | | ϵ_{6D} | | N_{survive} | |
|------------------------------------------------------|--------------|--------------|--------------|--------------|-----------------|-------------|-------------------------|-------------------------|
| units | mm-rad | | mm | | mm ³ | | per 20k POT | |
| Particle Species | μ^+ | μ^- | μ^+ | μ^- | μ^+ | μ^- | μ^+ | μ^- |
| At End of Rotator | 15.66 | 15.54 | 30.06 | 27.71 | 7368 | 6690 | 4536 | 4553 |
| $R_{\text{edge}} = 3.21 \text{ m}$ | 16.62 | 15.22 | 34.62 | 28.13 | 7998 | 6166 | 4037 (89.0%) | 4177 (91.7%) |
| $R_{\text{edge}} = 4.25 \text{ m}$ | 15.99 | | 35.71 | | 8316 | | 4194 | |
| $R_{\text{edge}} = 5.28 \text{ m}$ | 15.35 | | 36.87 | | 8504 | | 4282 | |
| $R_{\text{edge}} = 6.32 \text{ m}$ | 15.16 | 15.35 | 38.28 | 34.15 | 8753 | 7944 | 4311 (95.0%) | 4466 (98.1%) |
| $R_{\text{edge}} = 7.36 \text{ m}$ | 15.20 | 15.29 | 39.32 | 35.37 | 9051 | 8215 | 4282 | 4463 |
| $R_{\text{edge}} = 8.39 \text{ m}$ | 15.35 | | 41.73 | | 9780 | | 4279 | |
| $R_{\text{edge}} = 9.43 \text{ m}$ | 15.59 | | 43.11 | | 10,320 | | 4257 | |
| Acceptance of Katsuya's HCC | 20.4 | | 42.8 | | 12,900 | | | |

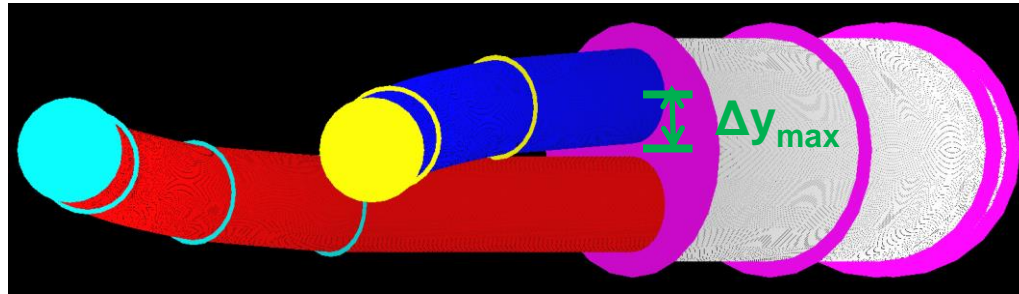
Results in green rows are at the end of charge splitter using the configuration identified by Redge.

Ecalc9f cuts: (Effectively momentum only)

- 175 MeV/c < p < 375 MeV/c
- Atrans < 1m, Along < 0.92244 m ← none for 325 MHz

Recall that these simulations were performed on independent configurations specific to a charge sign. A separate study of the geometry reveals a constraint on the outer radius of the downstream coils to be:

$$R_{\text{outer}} < 29.8 \text{ cm}$$

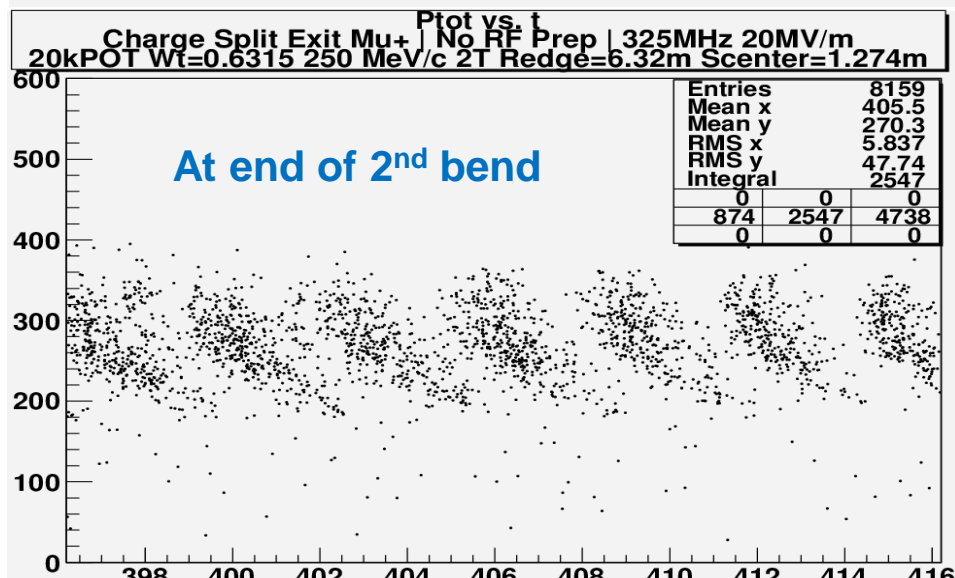
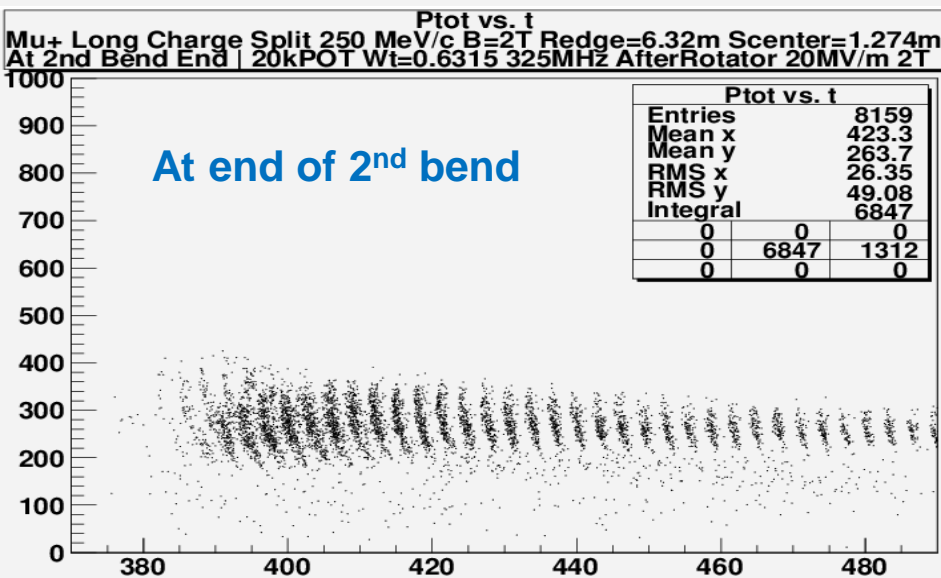
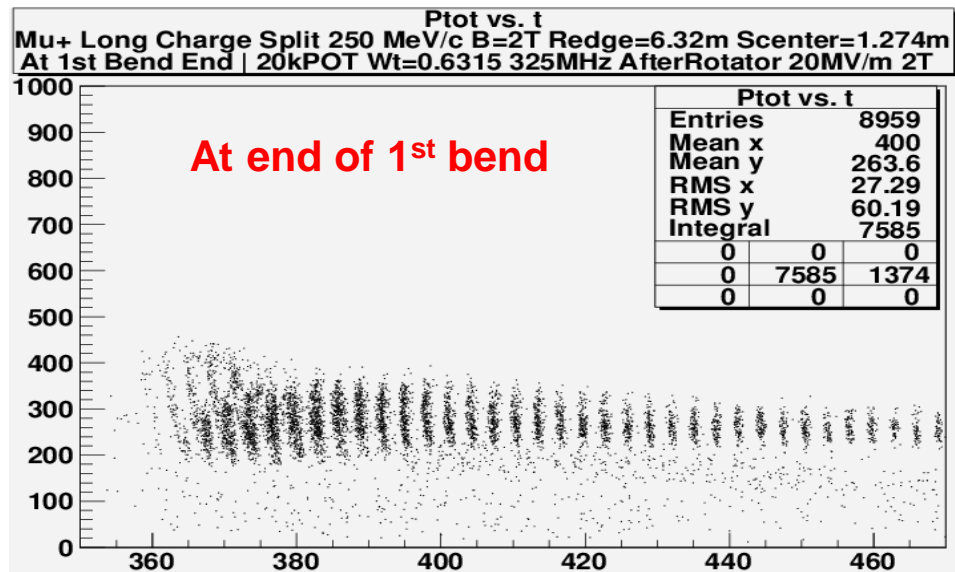
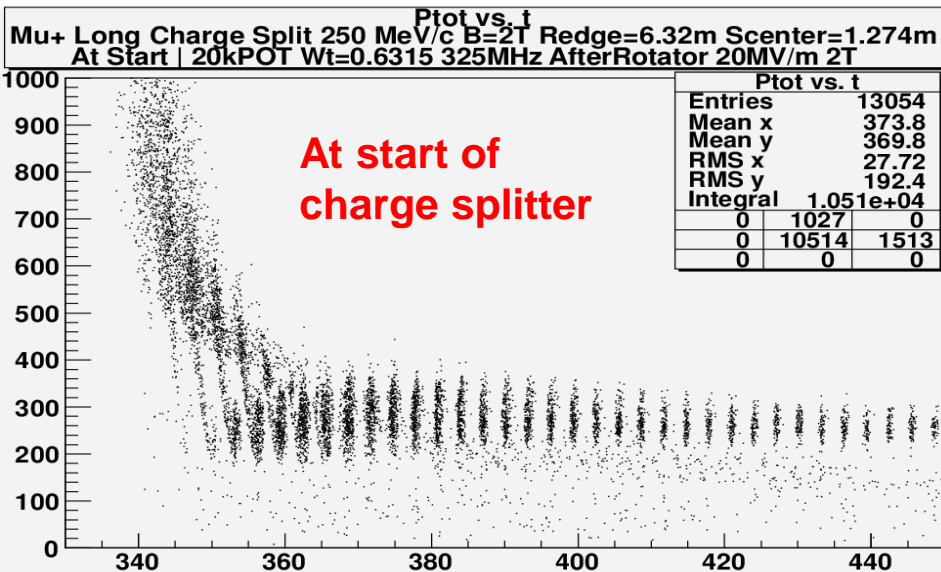


Distortion of the Longitudinal Dynamics at CS Exit

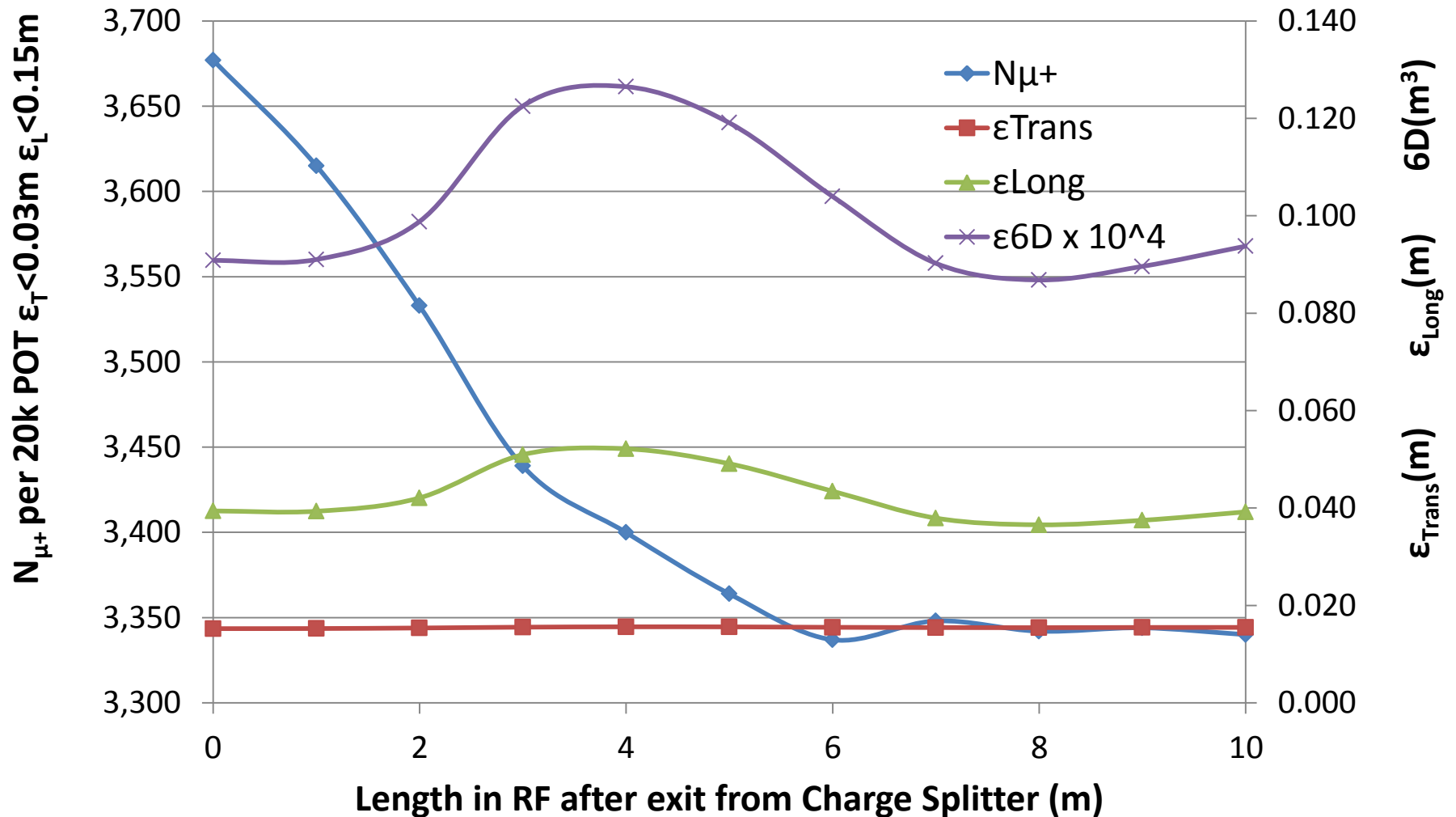
Ecalc9f calculations at the end of the charge splitter indicate a high rate of muons (95% μ^+ & 98% μ^-) that fit within the acceptance of the HCC.

However, inspection of the longitudinal dynamics at the exit reveal losses in the downstream RF capture.

P(MeV/c) vs. T(nsec) for $R_{\text{edge}} = 6.32\text{m}$



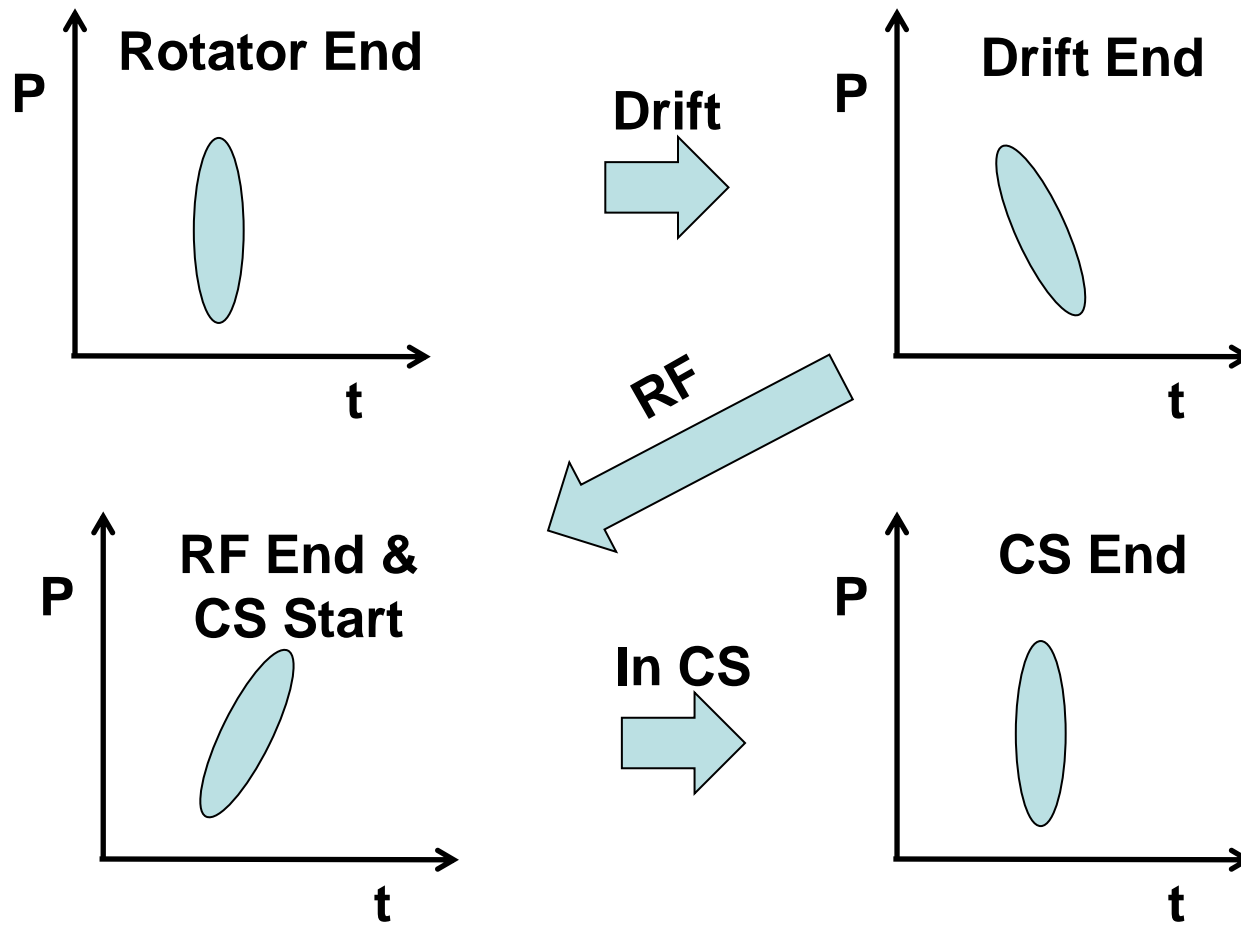
Rate and Emittances of Mu+ in RF After Charge Separator



$$\Delta N_{\mu^+}(\text{RF capture}) = (3350 - 3677) / 3677 = -9\%$$

Longitudinal Phase Space Preparation

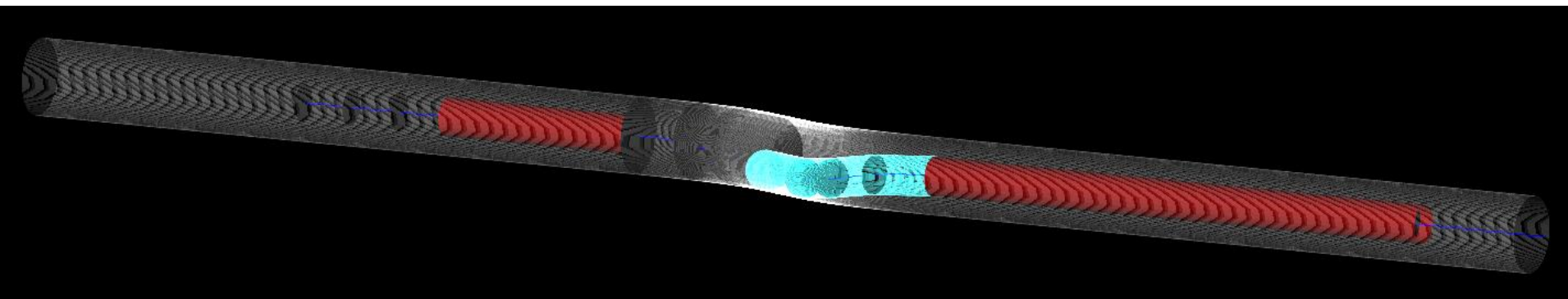
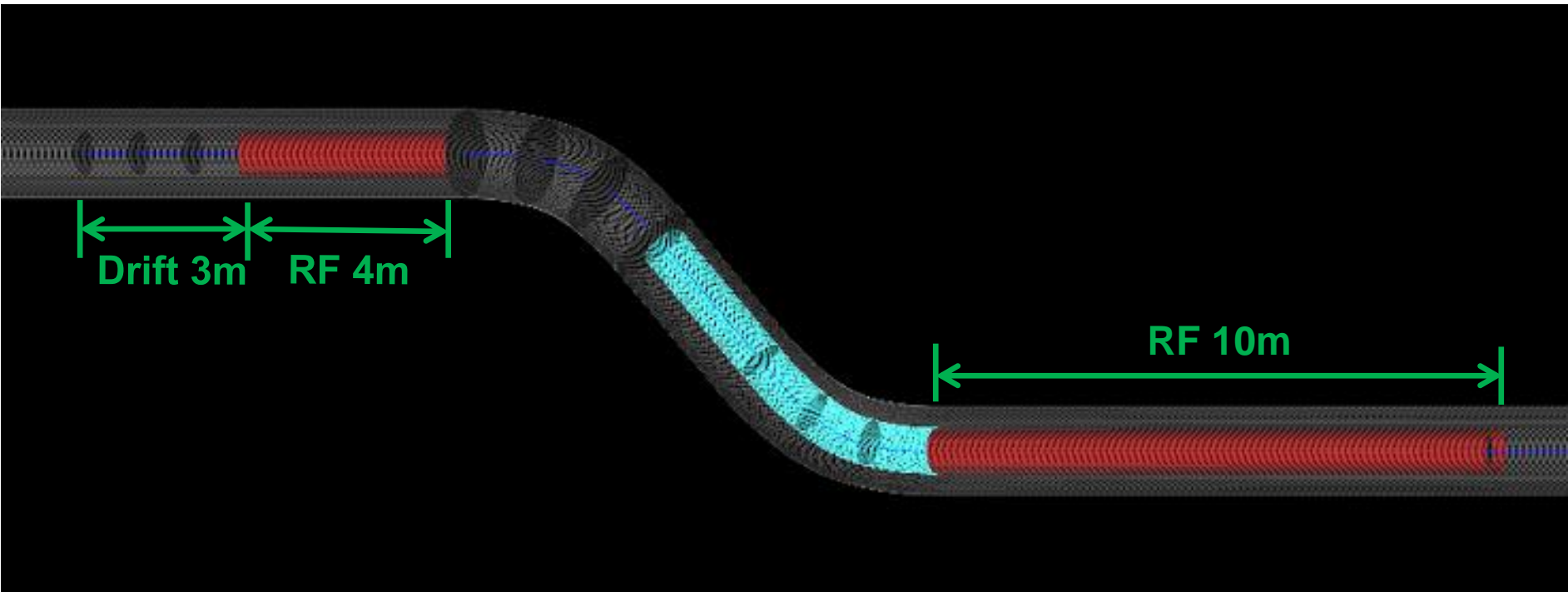
A solution to the longitudinal distortion created by the lack of RF in the charge separator is to prepare the beam upstream.



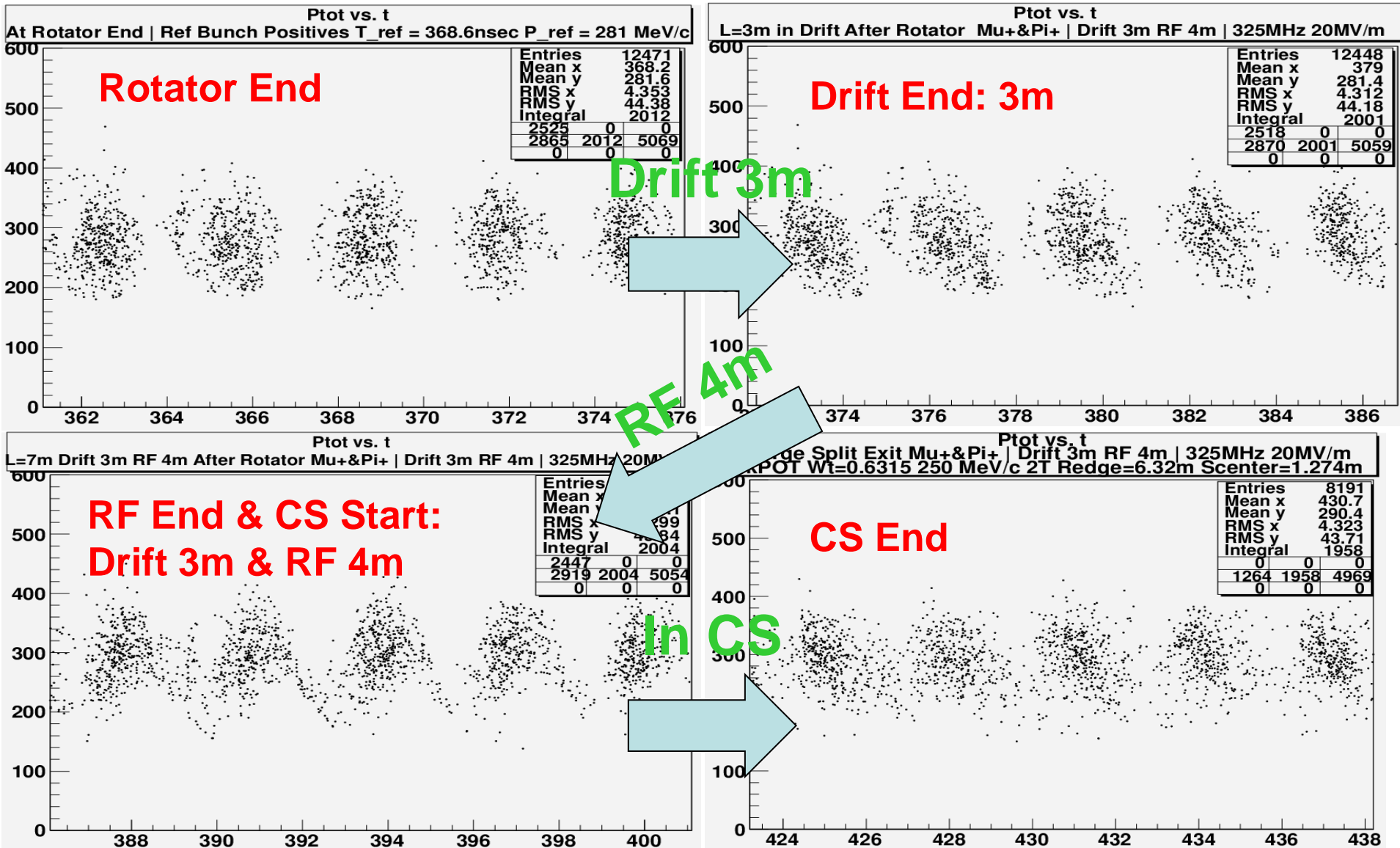
RF Prep Configurations

| Drift (m) | RF (m) |
|-----------|--------|
| 2 | 3 |
| 2 | 4 |
| 2 | 5 |
| 3 | 3 |
| 3 | 4 |
| 3 | 5 |
| 4 | 3 |
| 4 | 4 |
| 4 | 5 |

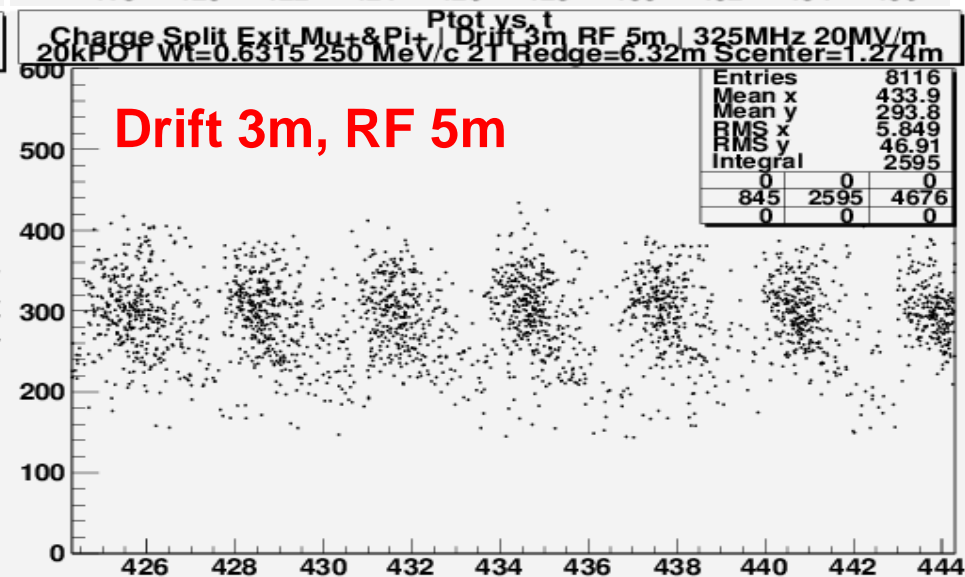
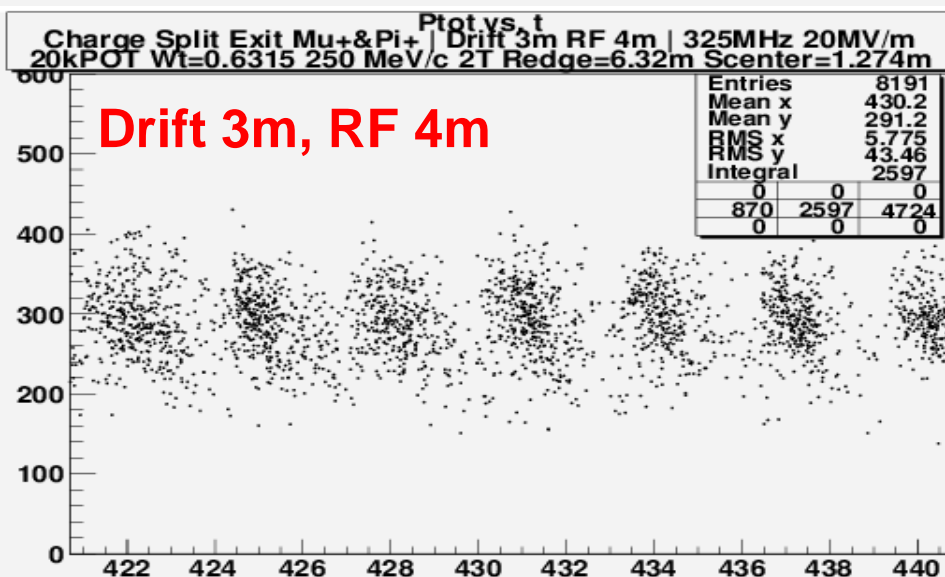
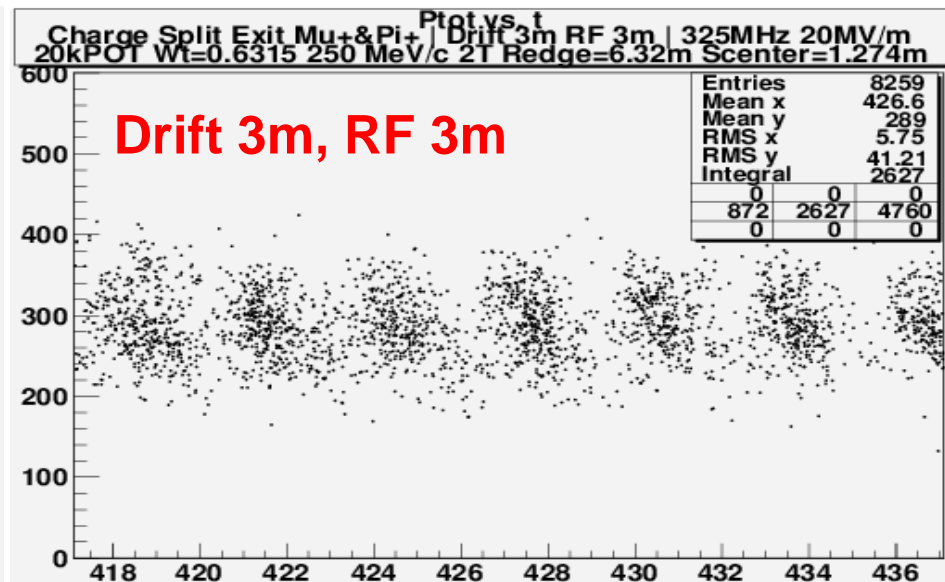
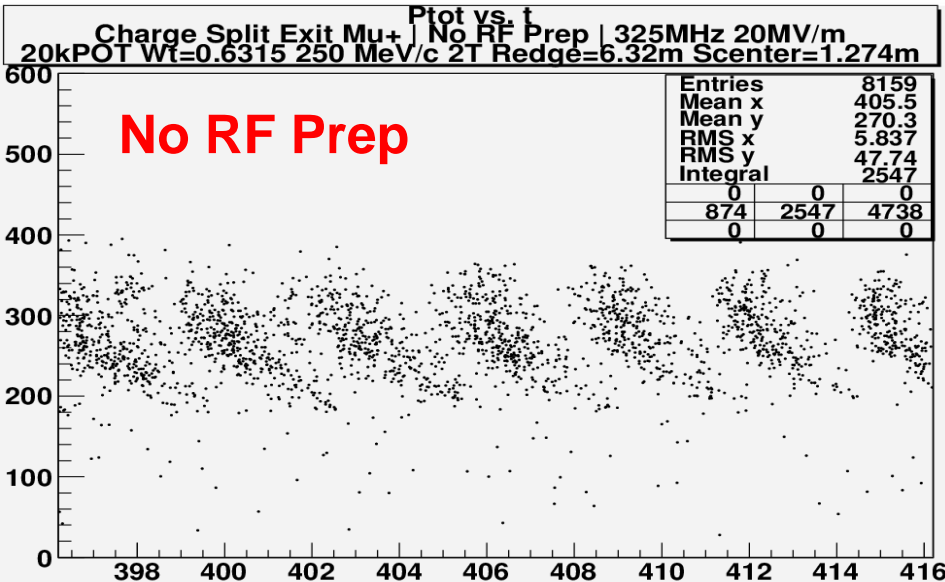
Drift 3m & RF 4m



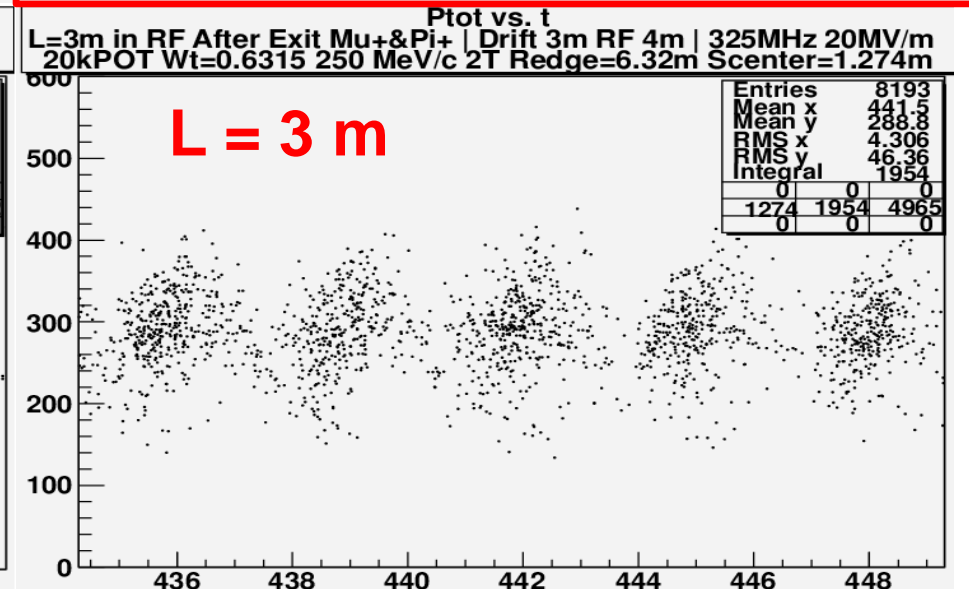
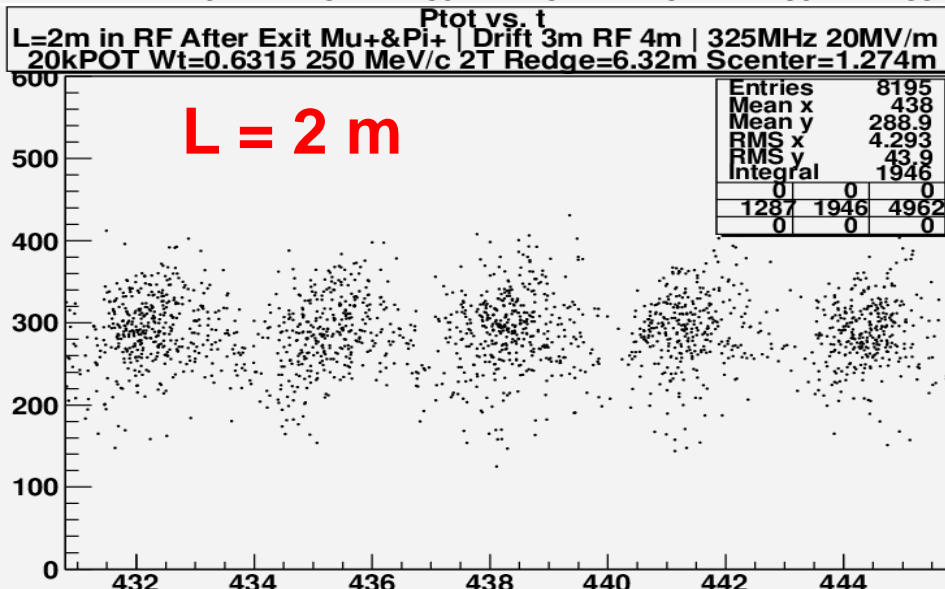
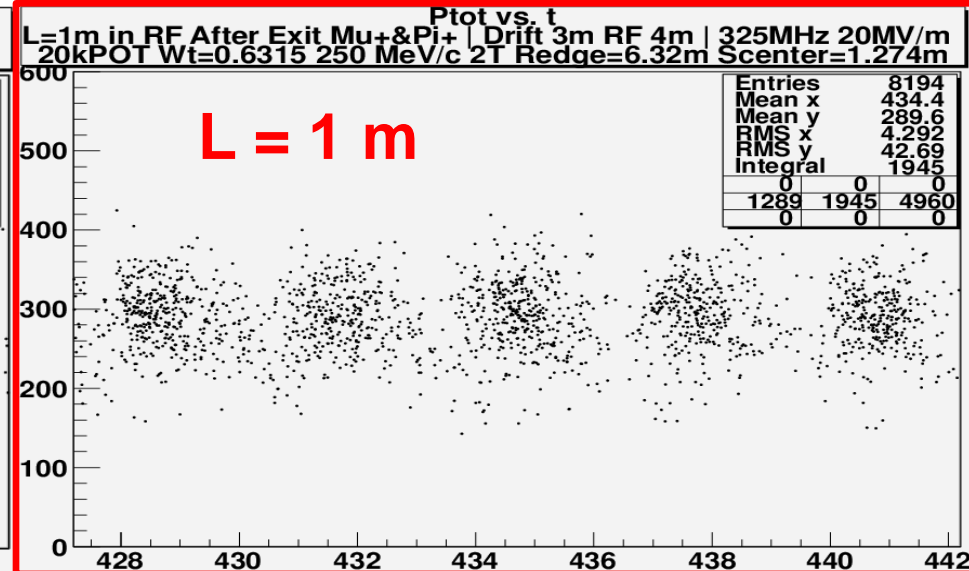
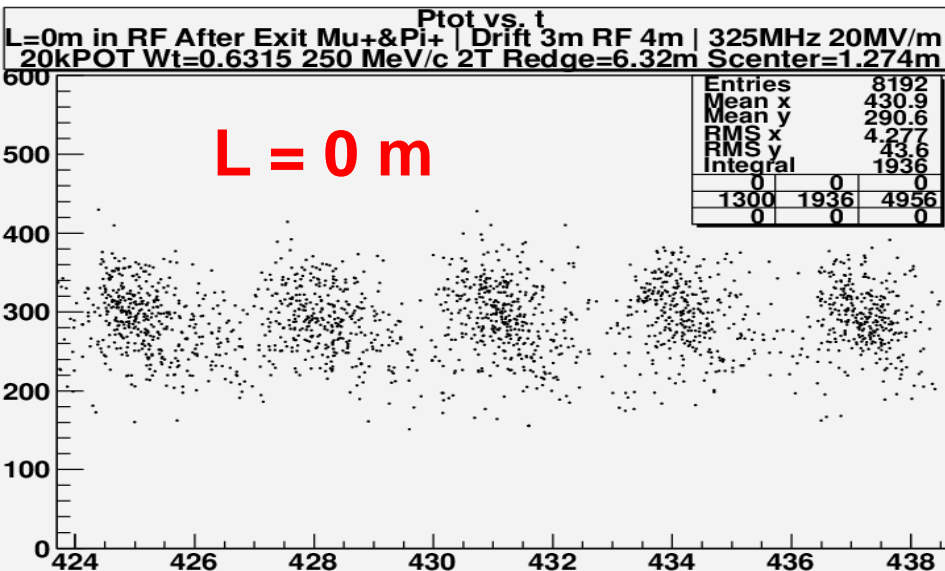
P(MeV/c) vs. T(nsec) for Mu+ thru Prep and Charge Splitter



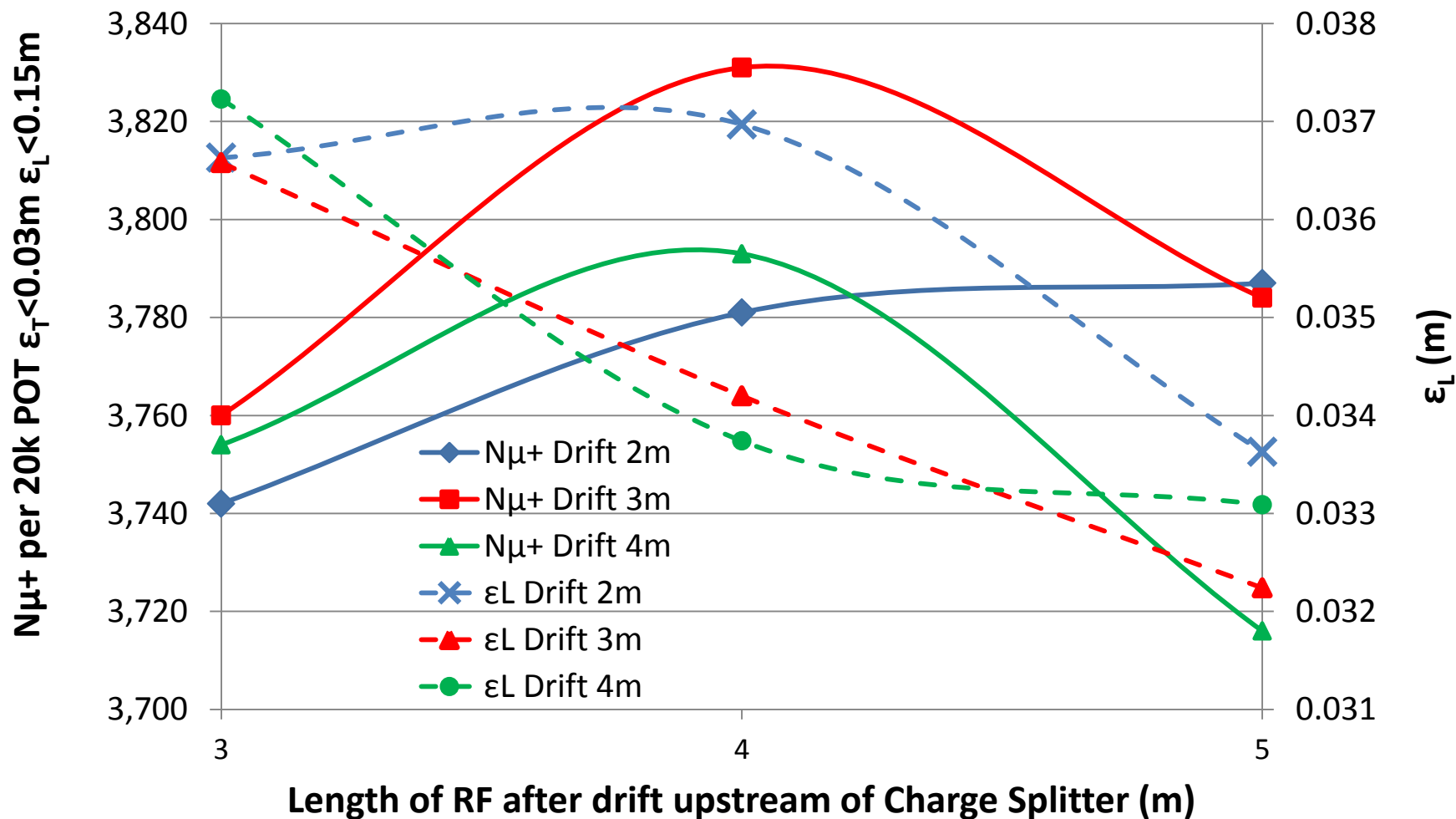
P(MeV/c) vs. T(nsec) for Mu+ at End of Charge Splitter



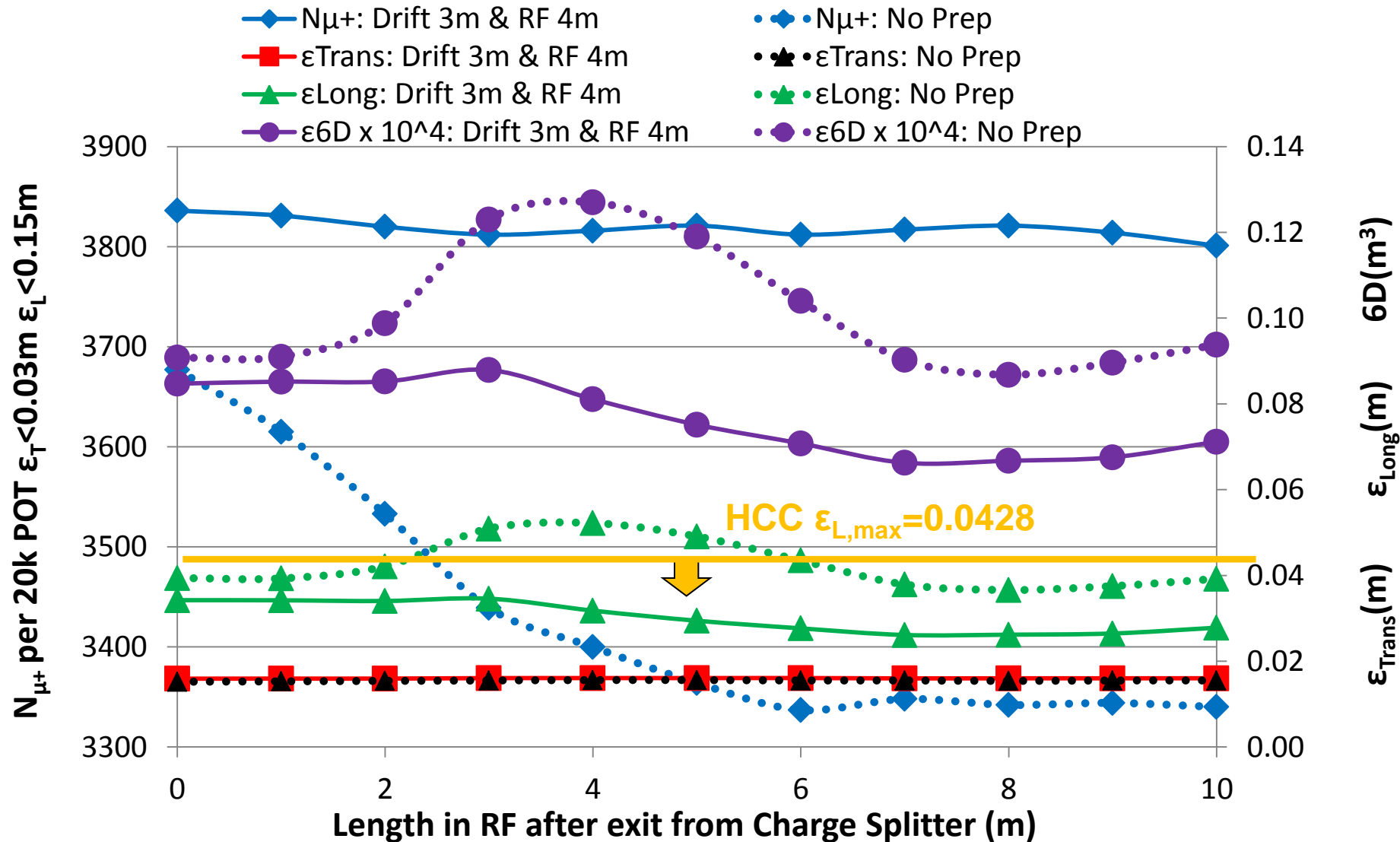
RF Capture for Mu+ at end of Charge Splitter (Drift 3m & RF 4m)



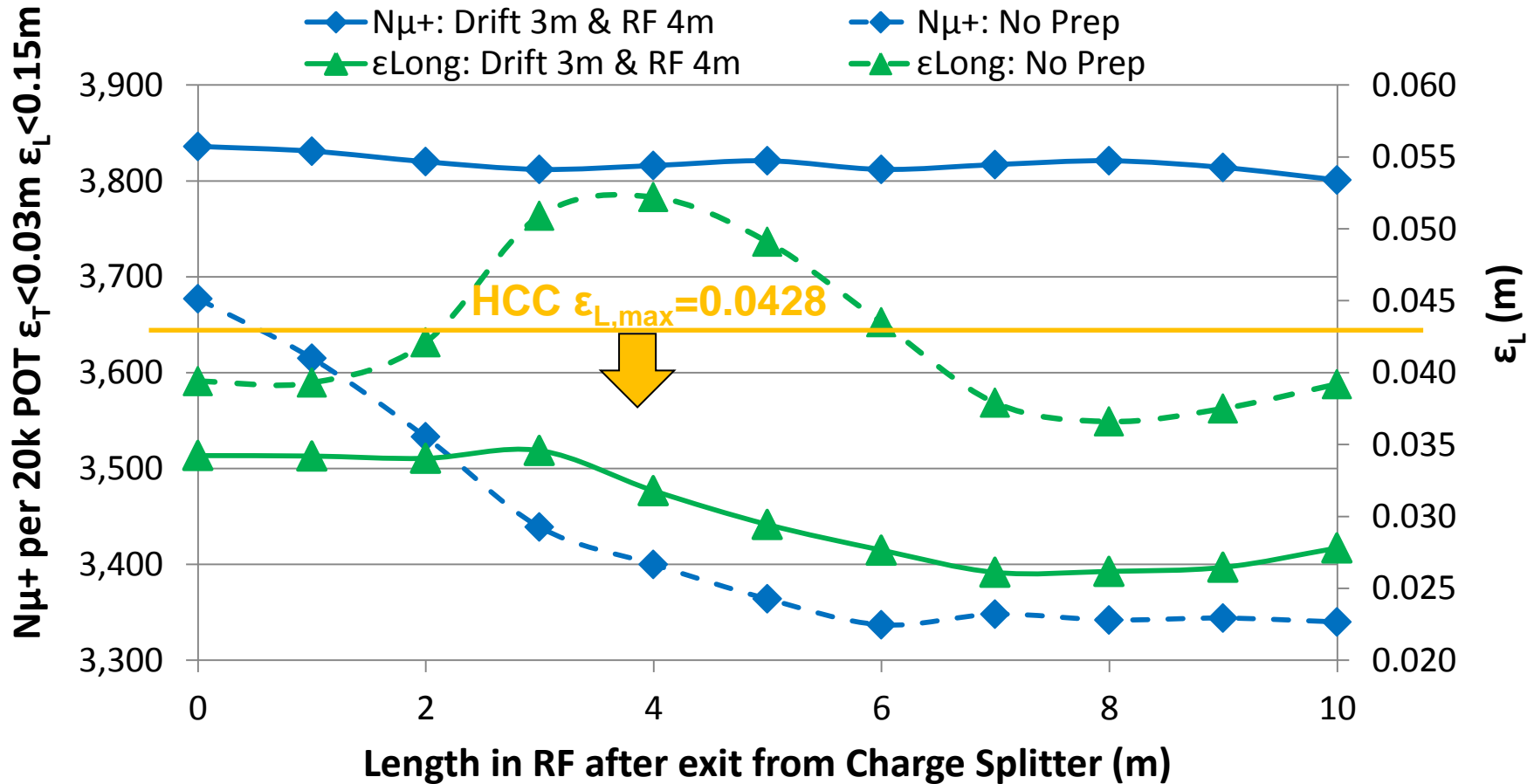
Rate and Longitudinal Emittance of Mu+ at 1m Past End of Charge Separator for Various RF Preparatory Configurations



Improvement in Rate and Emittances of Mu+ in RF After Charge Separator With Upstream Preparation



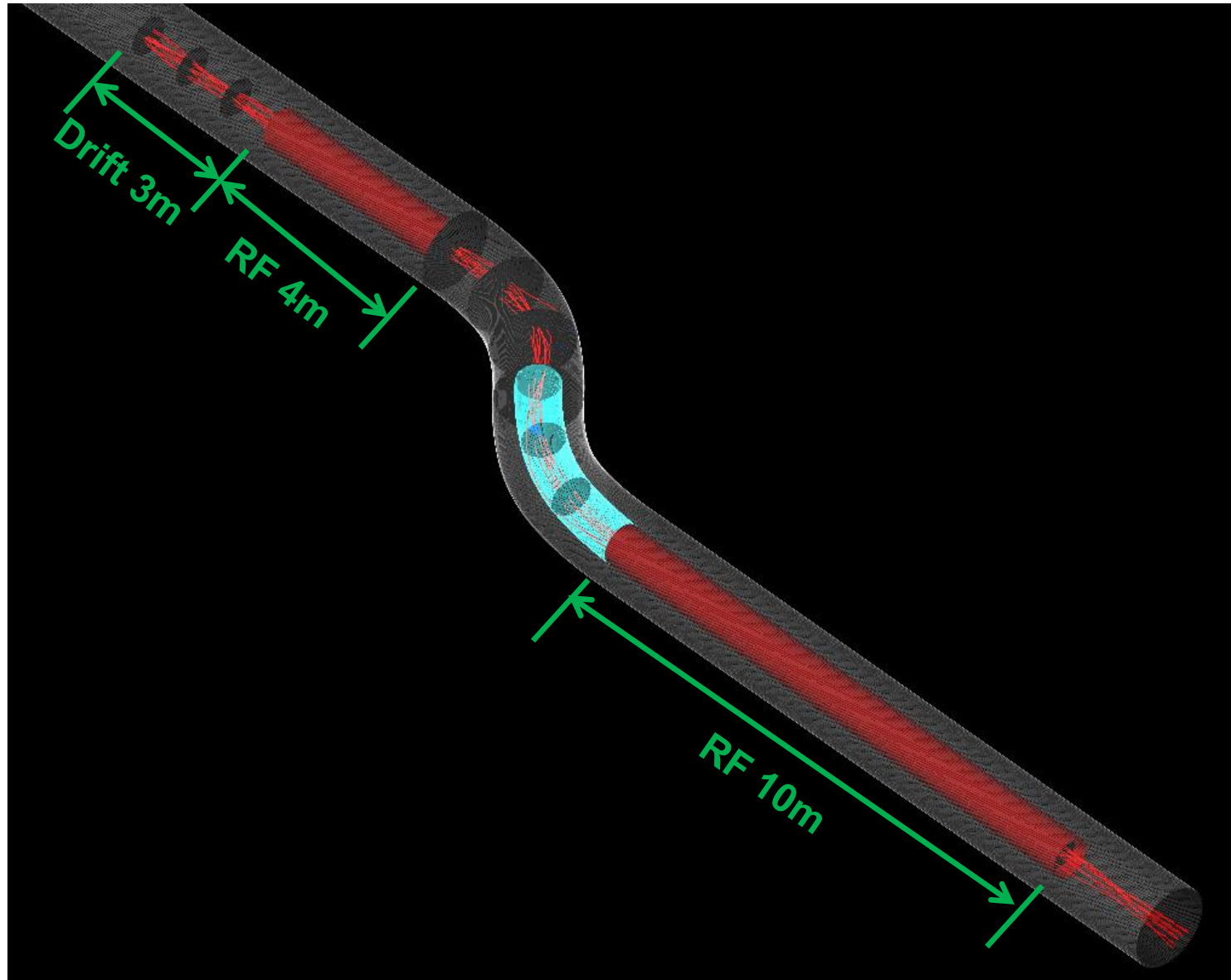
Improvement in Rate and Longitudinal Emittance of Mu+ in RF After Charge Separator With Upstream Preparation



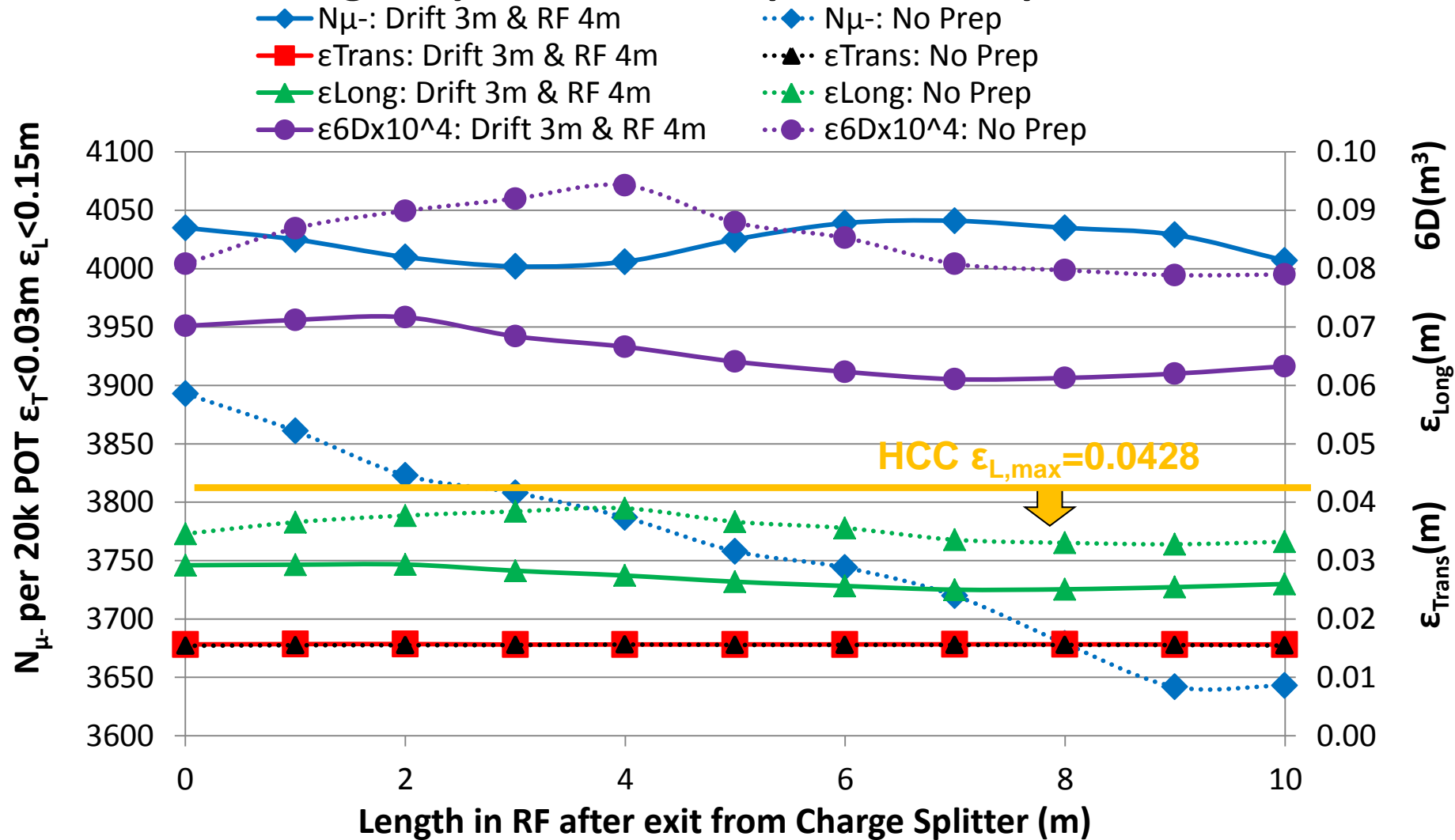
Effect of RF prep w/ 3m drift & 4m RF:

1. ϵ_L stays within the HCC acceptance.
2. Rate increase of $(3831-3342)/3342=14.6\%$

Analysis of Mu-'s

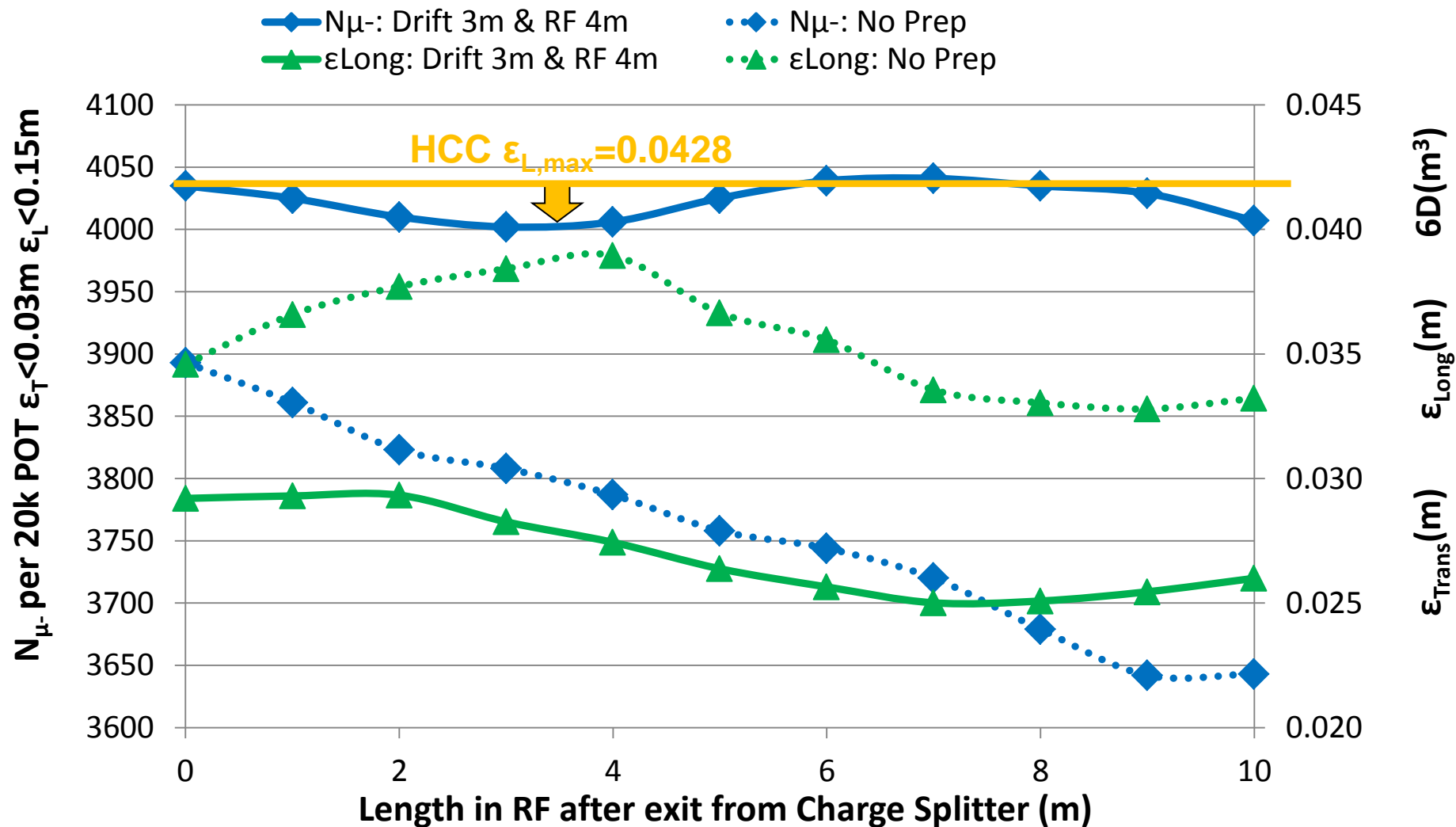


Improvement in Rate and Emittances of Mu- in RF After Charge Separator With Upstream Preparation



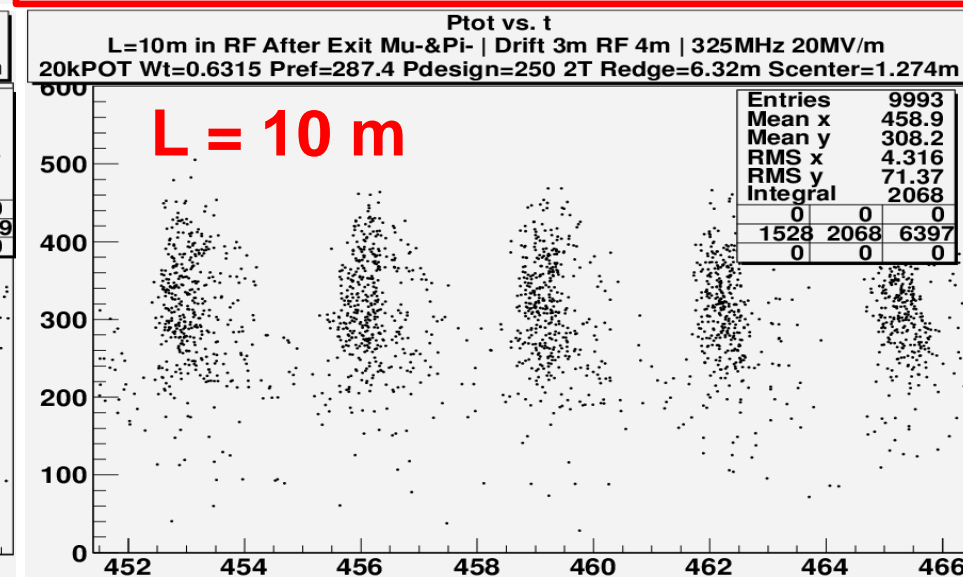
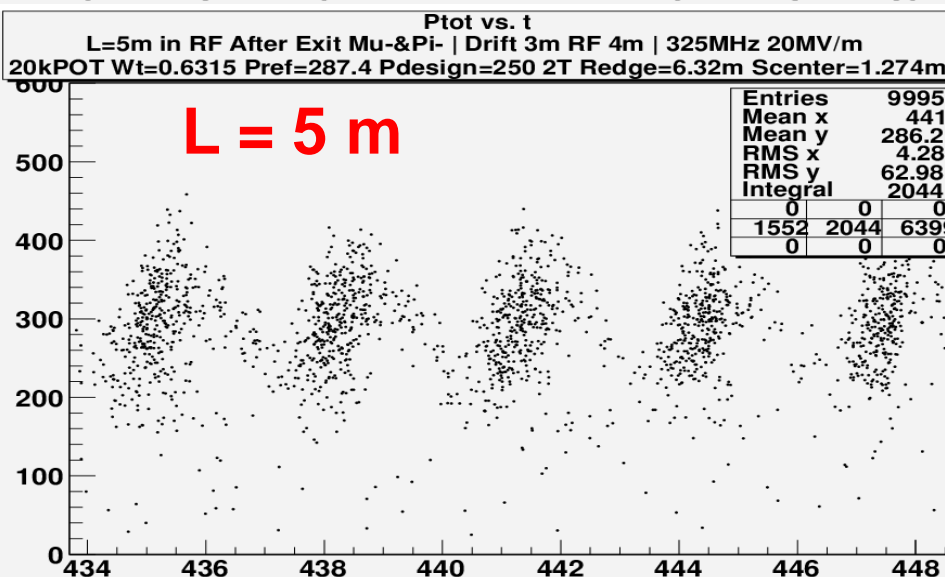
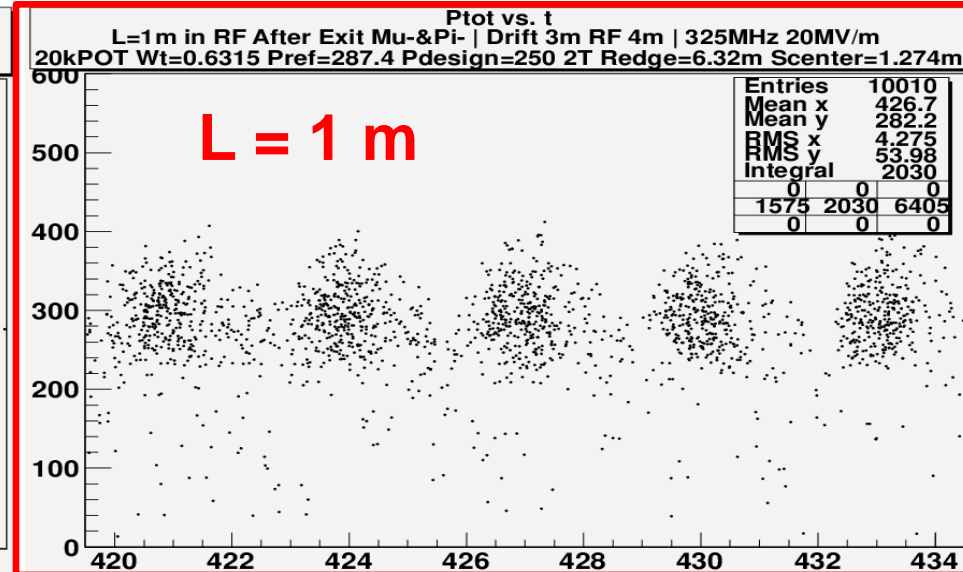
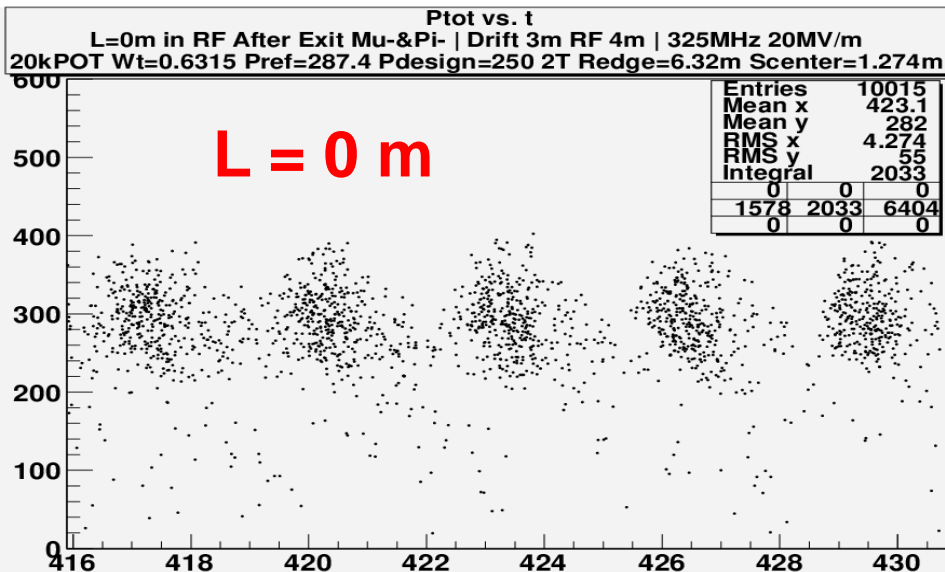
Preparation increases rate by $\sim (4025-3650)/3650=10\%$

Improvement in Rate and Longitudinal Emittance of Mu+ in RF After Charge Separator With Upstream Preparation



Preparation increases rate by $\sim (4025-3650)/3650=10\%$

RF Capture for **Mu-** at end of Charge Splitter (Drift 3m & RF 4m)



Results

| | ϵ_T | | ϵ_L | | ϵ_{6D} | | N_{survive} | |
|--------------------------------------------|--------------|---------|--------------|---------|-----------------|---------|----------------------|---------------|
| units | mm-rad | | mm | | mm ³ | | per 20k POT | |
| Particle Species | μ^+ | μ^- | μ^+ | μ^- | μ^+ | μ^- | μ^+ | μ^- |
| At End of Rotator [1] | 15.66 | 15.54 | 30.06 | 27.71 | 7368 | 6690 | 4536 | 4553 |
| At End of Rotator [2] | 15.66 | 15.54 | 30.06 | 27.71 | 7368 | 6690 | 4383 | 4444 |
| At End of Rotator [3] | 15.66 | 15.54 | 30.06 | 27.71 | 7368 | 6690 | 4118 | 4221 |
| Redge = 6.32 m @ 1m Drift 3m; RF 4m [3] | 15.94 | 15.69 | 34.2 | 29.30 | 8519 | 7122 | 3831 (-7%) | 4025 (-5%) |
| Acceptance of Katsuya's HCC | 20.4 | | 42.8 | | 12,900 | | | |

[1] Original Ecalc9f cuts: (Effectively none)

- Atrans < 1m;
- Along < 0.92244 m ← none for 325 MHz

[2] Loose Ecalc9f cuts: (longitudinal cut)

- Atrans < 0.3 m; same as aperture, so effectively none.
- Along < 0.2 m; used by Dave N.

[3] Tight Ecalc9f cuts: (longitudinal cut)

- Atrans < 0.3 m; same as aperture, so effectively none.
- Along < 0.15 m; used by Dave N.

Results

Particle data files of the Charge Separator output in g4bl and for009 formats are available at NERSC at:

/global/project/projectdirs/map/Users/yosh1/ChargeSeparatorOutput/<dir w/ latest date>

```
yosh1@hopper04:/global/project/projectdirs/map/Users/yosh1/ChargeSeparatorOutput> pwd
```

```
/global/project/projectdirs/map/Users/yosh1/ChargeSeparatorOutput
```

```
yosh1@hopper04:/global/project/projectdirs/map/Users/yosh1/ChargeSeparatorOutput> ll
```

```
total 640
```

```
drwxr-sr-x 3 yosh1 map 131072 2013-08-28 13:11 20130827\_Old
```

```
drwxr-sr-x 3 yosh1 map 131072 2013-09-06 08:34 20130828
```

```
-rwxr-xr-x 1 yosh1 map 127 2013-08-28 13:56 ReadMe
```

```
yosh1@hopper04:/global/project/projectdirs/map/Users/yosh1/ChargeSeparatorOutput/20130828> ll
```

```
total 10880
```

```
drwxr-sr-x 3 yosh1 map 131072 2013-08-28 13:12 DavesFrontEnd
```

```
-rwxr-xr-x 1 yosh1 map 1188347 2013-08-28 13:12 for009\_z=1m\_Positives.txt
```

```
-rwxr-xr-x 1 yosh1 map 1897441 2013-08-28 13:22 for009\_z=1m\_Positives\_ZaxisZ0.txt
```

```
-rwxr-xr-x 1 yosh1 map 2179333 2013-08-28 13:12 for009\_z=1m\_RefChangedToMuPlus\_Negatives.txt
```

```
-rwxr-xr-x 1 yosh1 map 2174283 2013-08-28 13:32 for009\_z=1m\_RefChangedToMuPlus\_NegativesZaxisZ0.txt
```

```
-rwxr-xr-x 1 yosh1 map 770875 2013-08-28 13:12 g4blDataFile\_z=1m\_NoRef\_Negatives.txt
```

```
-rwxr-xr-x 1 yosh1 map 716536 2013-08-28 13:32 g4blDataFile\_z=1m\_NoRef\_Negatives\_ZaxisZ0.txt
```

```
-rwxr-xr-x 1 yosh1 map 676766 2013-08-28 13:12 g4blDataFile\_z=1m\_NoRef\_Positives.txt
```

```
-rwxr-xr-x 1 yosh1 map 630126 2013-08-28 13:22 g4blDataFile\_z=1m\_NoRef\_Positives\_ZaxisZ0.txt
```

```
-rwxr-xr-x 1 yosh1 map 889 2013-09-06 08:34 ReadMe
```


Suggestions to improve next iteration of designing the Charge Separator

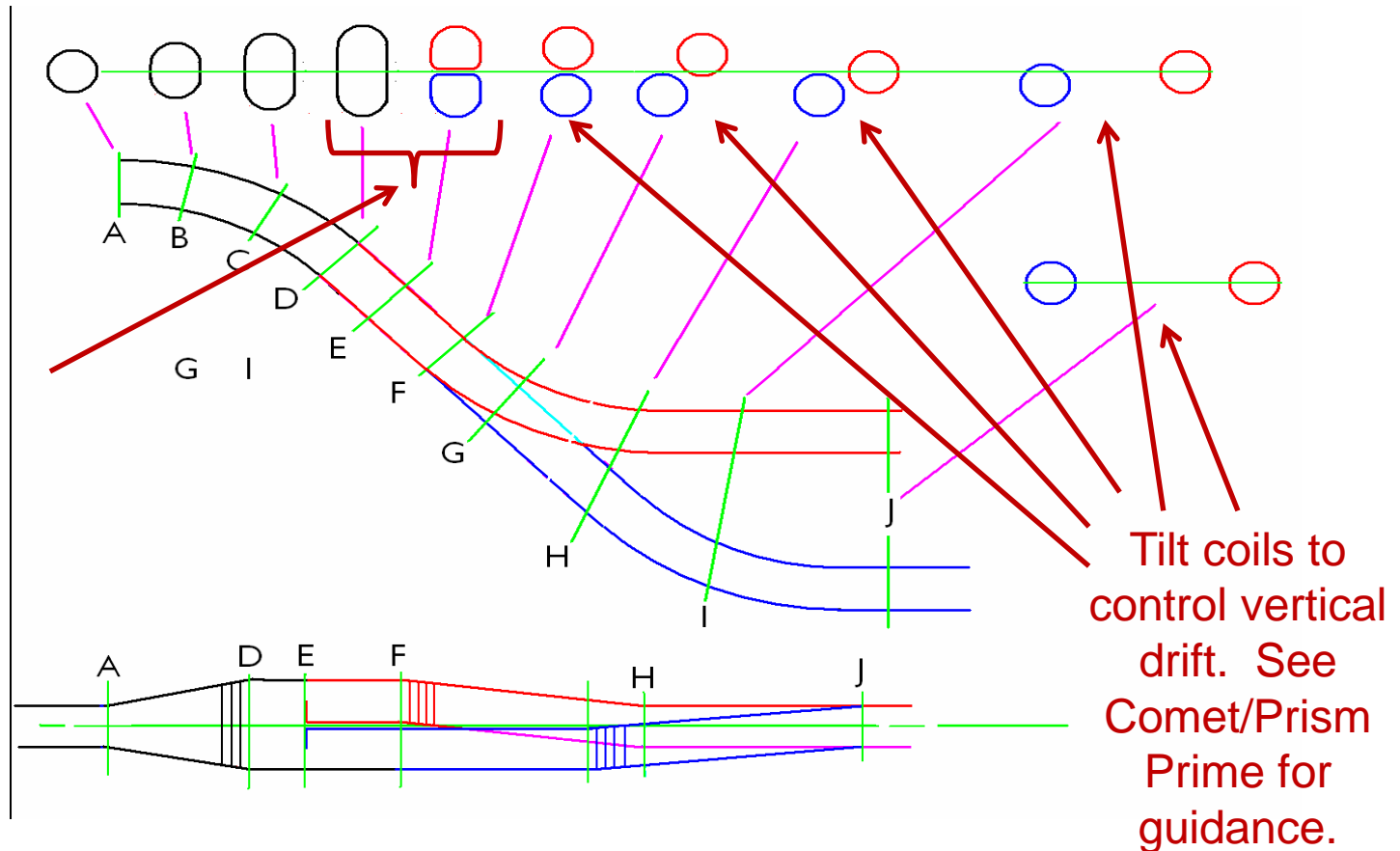
- Design the charge splitter for the momenta out of the front end, not what the front end thinks it should be.
 - $P_z(\mu^+ \text{ refBunch}) = 278 \text{ MeV}/c$, not 250
- May want to push μ^- 's through the longer path, since it has the lower starting $\epsilon_{\text{longitudinal}}$.

| | ϵ_T | | ϵ_L | | ϵ_{6D} | | N_{survive} | |
|-----------------------------|--------------|---------|--------------|--------------|-----------------|---------|----------------------|---------|
| units | mm-rad | | mm | | mm ³ | | per 20k POT | |
| Particle Species | μ^+ | μ^- | μ^+ | μ^- | μ^+ | μ^- | μ^+ | μ^- |
| At End of Rotator [3] | 15.66 | 15.54 | 30.06 | 27.71 | 7368 | 6690 | 4118 | 4221 |
| Acceptance of Katsuya's HCC | 20.4 | | 42.8 | | 12,900 | | | |

- Use same rf timing in the preparation for both signs for consistency.
- Vertically displaced coils may be useful. However, analytic theory not readily available.
 - Tilting vertically displaced coils should allow control to direct particles on the usual bent solenoid trajectory.

Suggestions to improve next iteration of designing the Charge Separator

Consider use of D shaped coils at transition at end of first bend.
(Bob Palmer)



G4beamline doesn't support coils that are not circular.

1. So, Tosca or some other tool that generates magnetic fields will need to be employed.
2. Or, G4beamline could be enhanced to expedite the design.

Suggestions to improve next iteration of designing the Charge Separator

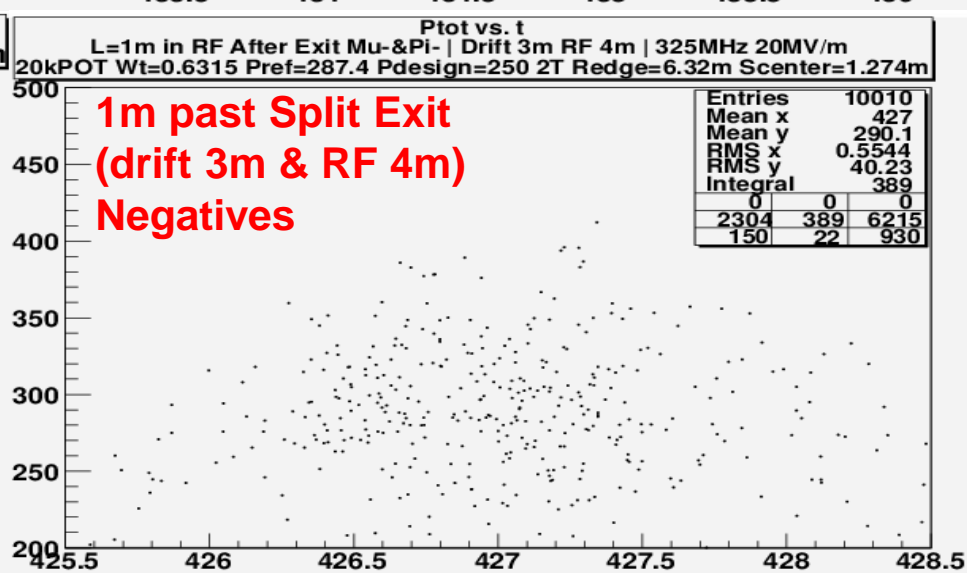
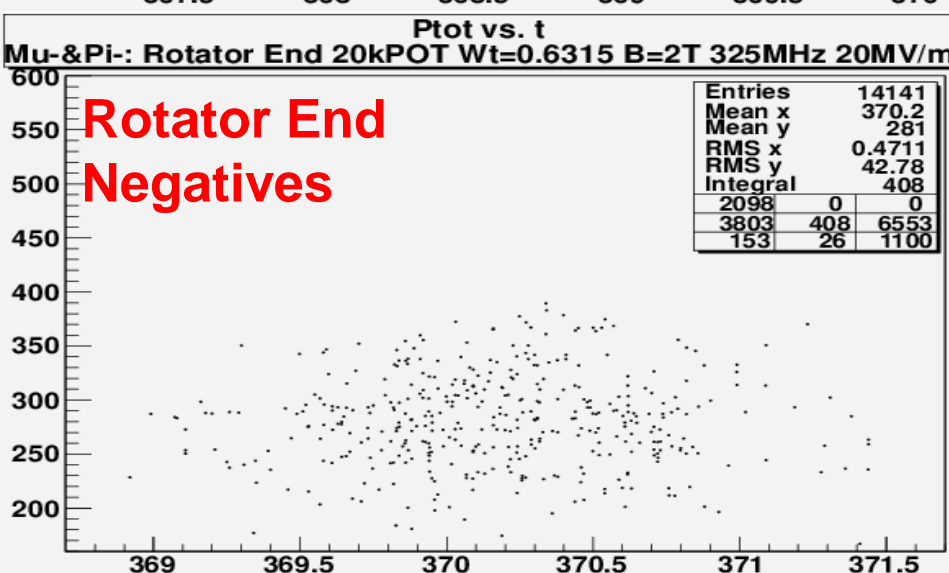
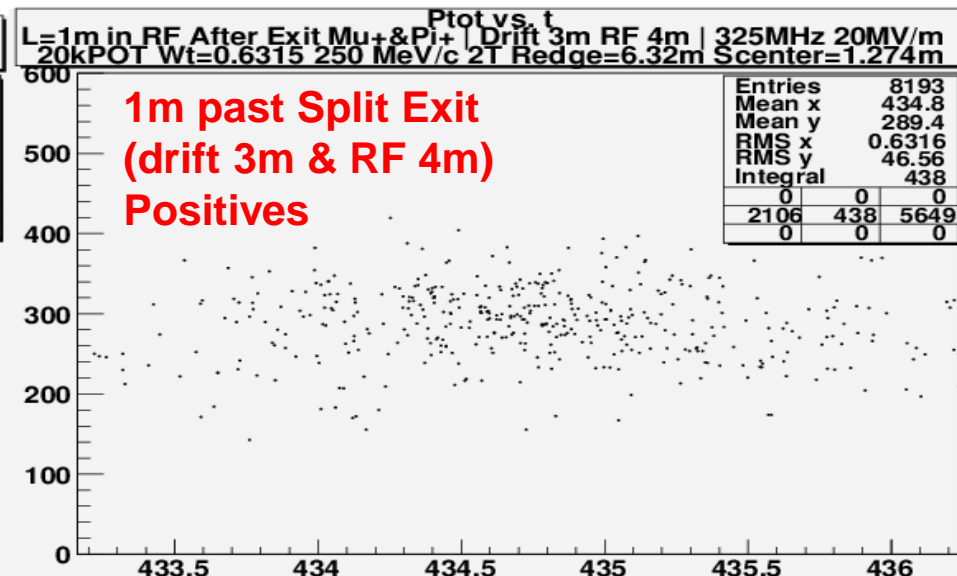
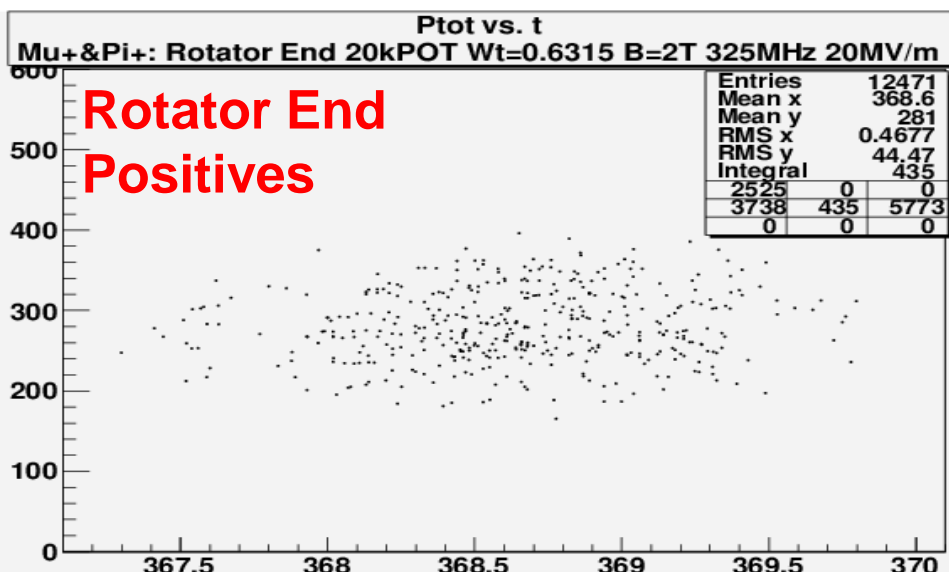
- Use results of studies that match out of the Charge Separator to decide the amount of acceleration provided to the bunches during the preparation.
 - Since ϵ_L is large for at least one sign coming out of the Charge Separator, we are considering the use of a RF phase that is smaller than that needed to fully replenish energy loss from the cooling material. Consequences are:
 - Larger RF bucket.
 - Energy of reference hones in on the region with better cooling performance while cooling particles near the edge of the enlarged RF bucket.

Summary & Future

- We have generated simulated particles that are representative of that having gone through a charge separator, which increases the reality of results in designs of downstream systems, say a 6D cooling channel.
- These simulated particles are publicly available at NERSC.
- We created a list of suggested improvements to design a real charge separator system.
- The next task for our team is to use the simulated particles in the design of a matching section into the HCC.

Back up

P(MeV/c) vs. T(nsec) Before and After the Charge Splitter



Expected Cooling Performance

- The 6D cooling reach of the HCC has not been revisited recently.

Parameters of the 7 HCC cooling channel segments used by Yonehara [IPAC10, MOPD076]. All Z values (except for 0) refer to the end of a segment with segment number designated by unit value.

| | Z | b_φ | | b_z | λ_{HCC} | ν | ε_T | ε_L | ε_{6D} | E |
|------|----------|----------------------|------|----------------------|------------------------|----------|----------------------|----------------------|-----------------------|--------------|
| unit | m | T | T/m | T | m | GHz | mm rad | mm | mm3 | Transmission |
| 1 | 0 | 1.3 | -0.5 | -4.2 | 1.0 | 0.325 | 20.4 | 42.8 | 12900 | |
| 2 | 40 | 1.3 | -0.5 | -4.2 | 1.0 | 0.325 | 5.97 | 19.7 | 415.9 | 0.92 |
| 3 | 49 | 1.4 | -0.6 | -4.8 | 0.9 | 0.325 | 4.01 | 15.0 | 108 | 0.86 |
| 4 | 129 | 1.7 | -0.8 | -5.2 | 0.8 | 0.325 | 1.02 | 4.8 | 3.2 | 0.73 |
| 5 | 219 | 2.6 | -2.0 | -8.5 | 0.5 | 0.65 | 0.58 | 2.1 | 2.0 | 0.66 |
| 6 | 243 | 3.2 | -3.1 | -9.8 | 0.4 | 0.65 | 0.42 | 1.3 | 0.14 | 0.64 |
| 7 | 273 | 4.3 | -5.6 | -14.1 | 0.3 | 0.65 | 0.32 | 1.0 | 0.08 | 0.62 |
| 8 | 303 | 4.3 | -5.6 | -14.1 | 0.3 | 1.3 | 0.32 | 1.0* | 0.07 | 0.60 |

- Finding the 6D cooling reach of the HCC will probe lower momentum to find a configuration that supports a stable system with the lowest ϵ_{equil} .